REPORT NO. UMTA-MA-06-0025-80-2

# INCREASED RAIL TRANSIT VEHICLE CRASHWORTHINESS IN HEAD-ON COLLISION

## Volume II - Primary Collision

Edward E. Hahn
Steven C. Walgrave
Theodore Liber

IIT RESEARCH INSTITUTE
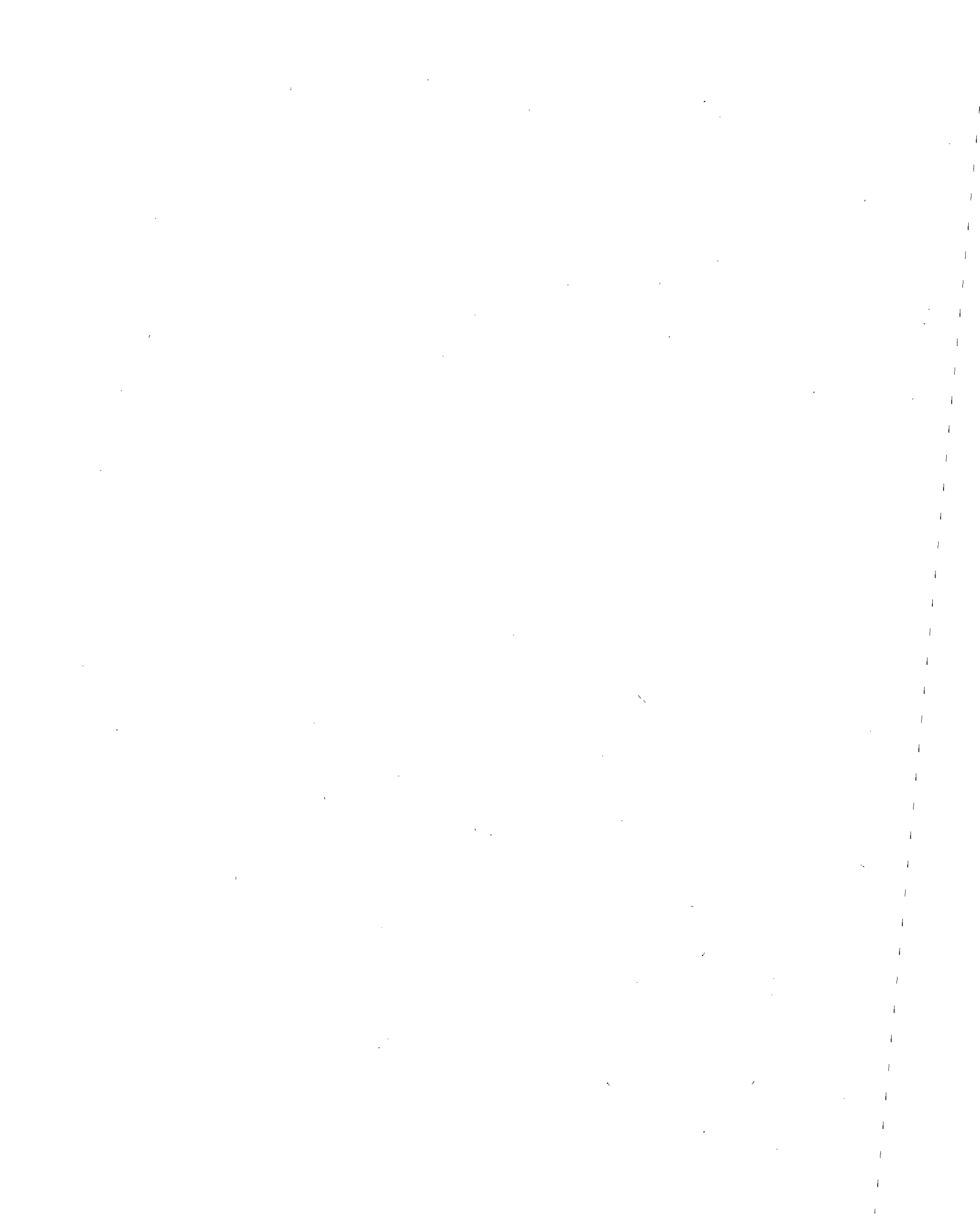10 West 35th Street
Chicago IL    60616

JUNE 1980
FINAL REPORT

Prepared by

# GENERAL DISCLAIMER

| 1. Report No. <br> UMTA-MA-06-0025-80-2 | 2. Government Accession No. | 3. Recipient's Catalog No. <br> PB80  205743 | | |
|---|---|---|---|---|
| 4. Title and Subtitle <br><br> INCREASED RAIL TRANSIT VEHICLE CRASHWORTHINESS IN HEAD-ON COLLISIONS <br> Volume II: PRIMARY COLLISION | | 5. Report Date <br> June 1980 | | |
| | | 6. Performing Organization Code | | |
| 7. Author(s) <br> Edward E. Hahn, Steven C. Walgrave, and Theodore Liber | | 8. Performing Organization Report No. <br> DOT-TSC-UMTA-80-17,II | | |
| 9. Performing Organization Name and Address <br> IIT Research Institute* <br> 10 West 35th Street <br> Chicago, Illinois 60616 | | 10. Work Unit No. (TRAIS) <br> MA-06-0025(UM904/R0734) | | |
| | | 11. Contract or Grant No. <br> DOT-TSC-1052-2 | | |
| | | 13. Type of Report and Period Covered <br> Final Report <br> June 1975 – June 1978 <br> Volume II of IV | | |
| 12. Sponsoring Agency Name and Address <br> U.S. Department of Transportation <br> Urban Mass Transportation Administration <br> 400 Seventh Street, S.W. <br> Washington, DC 20590 | | | | |
| | | 14. Sponsoring Agency Code <br> UTD-30 | | |

15. Supplementary Notes

*under contract to:    U.S. Department of Transportation
Research and Special Programs Administration
Transportation Systems Center
Cambridge, Massachusetts 02142

16. Abstract

As systems manager for the Urban Mass Transportation Administration (UMTA) Rail System Supporting Technology Program, the Transportation Systems Center (TSC) is conducting research and development efforts directed toward the introduction of improved technology in urban rail system applications. As part of this program, TSC is conducting analytical and experimental studies toward improved safety in urban rail systems. A specific goal in this area of safety is to reduce the number of injuries that may result from the collision of two trains. In this report, Volume II, an analytical model in two dimensions, longitudinal and vertical, of the primary collision of two impacting urban railcar consists is formulated. This model includes the formulation of the leading cars developed in Part 1 of this program, and the distribution of mass and nonlinear force-deformation relationships existing among major structural sub-assemblages. This model also is capable of determining the extent of crushing and/or override suffered by the individual cars in the consists, as well as the time histories of displacement, velocity, and acceleration in both the longitudinal and vertical directions. Methods are developed for generating the dynamic force-deformation relationships for structural sub-assemblages comprising the critical modules of railcars. These methods include finite-element analysis, scale modeling, and full-scale testing procedures including specifications for required testing equipment and instrumentation. The finite element analytical method is utilized to generate the nonlinear force-deformation relationships among major components of a typical urban railcar. Other volumes are: Volume I: Initial Impact (UMTA-MA-06-0025-80-1); Volume III: Guidelines for Evaluation and Development of New Railcar Designs (UMTA-MA-06-0025-80-3); and Volume IV: IITRAIN Users' Manual (UMTA-MA-06-0025-80-4).

| 17. Key Words <br> Collisions; Commuter Rail Cars; Crashworthiness; Head-On Collisions; Impacts; Models; Primary Collisions; Railcar Crashworthiness; Rapid Transit Cars; Train Crashes; Transportation Safety | | 18. Distribution Statement <br><br> Available to the public through the National Technical Information Service, Springfield, Virginia 22161. | | |
|---|---|---|---|---|
| 19. Security Classif. (of this report) <br> Unclassified | | 20. Security Classif. (of this page) <br> Unclassified | 21. No. of Pages | 22. Price |

Form DOT F 1700.7 (8-72)      Reproduction of completed page authorized

# PREFACE

As systems manager for the Urban Mass Transportation Administration (UMTA) Rail System Supporting Technology Program, the Transportation Systems Center (TSC) is conducting research and development efforts directed toward the introduction of improved technology in urban rail system applications. As part of this program, TSC is conducting analytical and experimental studies toward improved safety in urban rail systems. A specific goal in this area of safety is to reduce the number of injuries that may result from the collision of two trains.

On 30 June 1975, TSC contracted with IIT Research Institute (IITRI) to perform this study to develop engineering methods and data pertaining to improved technology in urban rail systems which will lead to increased rail transit vehicle crashworthiness and passenger injury minimization. This final report is submitted in four volumes. Part 1 describes the results of Task 1 which is concerned with the initial impact of two transit cars. The results of Task 2 which is concerned with the primary collision of two impacting transit car consists are described in Part 2. Part 3 describes the results of Tasks 3 and 4 of this study which are concerned with prediction of passenger injury and guidelines for evaluation of railcar designs. The final volume is a manual containing a description of the organization and use of the IITRAIN computer code which was developed as a tool to help meet the goals of this contract.

Major IITRI contributors to the work covered in this report include Edward E. Hahn, Arne H. Wiedermann, Anatole Longinow, Robert W. Bruce and Steven C. Walgrave. The author takes this opportunity to acknowledge the contributions to this report made by Dr. A. Robert Raab, Mr. Samuel Polcari, Dr. Ming Chen, Mr. George Neat and Mr. Ronald Madigan of the U.S. Department of Transportation, TSC, Cambridge, Massachusetts.

**METRIC CONVERSION FACTORS**

## Approximate Conversions to Metric Measures

| Symbol | When You Know | Multiply by | To Find | Symbol |
|---|---|---|---|---|
| **LENGTH** | | | | |
| | inches | 2.5 | centimeters | cm |
| | feet | 30 | centimeters | cm |
| | yards | 0.9 | meters | m |
| | miles | 1.6 | kilometers | km |
| **AREA** | | | | |
| | square inches | 6.5 | square centimeters | cm² |
| | square feet | 0.09 | square meters | m² |
| | square yards | 0.8 | square meters | m² |
| | square miles | 2.6 | square kilometers | km² |
| | acres | 0.4 | hectares | ha |
| **MASS (weight)** | | | | |
| | ounces | 28 | grams | g |
| | pounds | 0.45 | kilograms | kg |
| | short tons (2000 lb) | 0.9 | tonnes | t |
| **VOLUME** | | | | |
| | teaspoons | 5 | milliliters | ml |
| | tablespoons | 15 | milliliters | ml |
| | fluid ounces | 30 | milliliters | ml |
| | cups | 0.24 | liters | l |
| | pints | 0.47 | liters | l |
| | quarts | 0.95 | liters | l |
| | gallons | 3.8 | liters | l |
| | cubic feet | 0.03 | cubic meters | m³ |
| | cubic yards | 0.76 | cubic meters | m³ |
| **TEMPERATURE (exact)** | | | | |
| | Fahrenheit temperature | 5/9 (after subtracting 32) | Celsius temperature | °C |

## Approximate Conversions from Metric Measures

| Symbol | When You Know | Multiply by | To Find | Symbol |
|---|---|---|---|---|
| **LENGTH** | | | | |
| mm | millimeters | 0.04 | inches | in |
| cm | centimeters | 0.4 | inches | in |
| m | meters | 3.3 | feet | ft |
| m | meters | 1.1 | yards | yd |
| km | kilometers | 0.6 | miles | mi |
| **AREA** | | | | |
| cm² | square centimeters | 0.16 | square inches | in² |
| m² | square meters | 1.2 | square yards | yd² |
| km² | square kilometers | 0.4 | square miles | mi² |
| ha | hectares (10,000 m²) | 2.5 | acres | |
| **MASS (weight)** | | | | |
| g | grams | 0.035 | ounces | oz |
| kg | kilograms | 2.2 | pounds | lb |
| t | tonnes (1000 kg) | 1.1 | short tons | |
| **VOLUME** | | | | |
| ml | milliliters | 0.03 | fluid ounces | fl oz |
| l | liters | 2.1 | pints | pt |
| l | liters | 1.06 | quarts | qt |
| l | liters | 0.26 | gallons | gal |
| m³ | cubic meters | 35 | cubic feet | ft³ |
| m³ | cubic meters | 1.3 | cubic yards | yd³ |
| **TEMPERATURE (exact)** | | | | |
| °C | Celsius temperature | 9/5 (then add 32) | Fahrenheit temperature | °F |

TABLE OF CONTENTS

LIST OF ILLUSTRATIONS

ILLUSTRATIONS (Concl)

LIST OF TABLES

# 1. INTRODUCTION

The collision of two consists of transit cars can be broken into three separate, but interdependent, phenomena: initial impact, primary collision, and secondary collision. Initial impact is concerned with the mechanics of the initial impact of the leading cars of two consists. The interaction of all of the cars and car components of two impacting consists comprise the primary collision. Secondary collisions include the interaction of passengers with the car components, passengers with passengers and passengers with other loose objects. This final report, submitted in four volumes, describes the results of the IIT Research Institute (IITRI) program which is concerned with the collision of transit car consists on straight level track. Part 1 of the final report is concerned with the initial impact of the leading cars of two consists. The results of the study of the primary collision of two impacting consists are given in Part 2, and Part 3 is concerned with secondary collisions including the prediction of passenger injury and guidelines for evaluation of new railcar designs. The final volume is a manual containing a description of the organization and use of the IITRAIN computer code which was developed as a tool to help meet the goals of this contract.

## 1.1 Program Objectives

The program objectives, as taken from the contract, are restated here.

Item 1a: Formulate an analytical model in two dimensions, longitudinal and vertical, of the leading cars of two impacting consists in sufficient detail to examine the mechanics of head-on initial impact on straight track. This model will include the distribution of mass in the cars as well as the nonlinear force-deformation relationships existing among major structural subassemblages. Consideration will be given to the shapes and configurations of the impacting surfaces and to the forces generated by

1

the impact. The model shall be capable of establishing the critical parameters which govern whether the cars crush, displace vertically and override, or crush with subsequent override.

Item 1b: Utilize the above analytical model of initial impact to assess impact controlling devices currently in service, such as anticlimbers, couplers and draft gears of various designs. This assessment shall uncover the critical parameters of such devices which govern whether the cars crush, displace vertically and override or crush with subsequent override. The contractor shall develop recommendations concerning future directions of effort in design of impact controlling devices which would be particularly pertinent to crashworthiness goals.

Item 1c: Develop an experimental test plan for the evaluation of the strength and effectiveness of future designs for impact controlling devices. These tests are to assure that the forces generated during impact do not produce structural failure of the impact controlling device or vertical misalignment and override of the car body. The test plan is to be sufficiently detailed so that all equipment, fixtures, instrumentation and procedures are completely described.

Item 2a: Develop an analytical model in two dimensions, longitudinal and vertical, of the primary collision of two impacting consists of urban railcars of similar and different configurations. This model will include the formulation of the leading cars developed in Part 1 of this program, as well as the distributions of mass and nonlinear force-deformation relationships existing among major structural subassemblages. This model shall be capable of determining the extent of crushing and/or override suffered by the individual cars in the consists, as well as the time histories of displacement, velocity, and acceleration in both the longitudinal and vertical directions.

Item 2b: Develop methods for generating the dynamic force-deformation relationships for structural subassemblages comprising the critical modules of railcars. These methods shall include

finite-element analysis, scale modeling and full-scale testing procedures including specifications for required testing equipment and instrumentation. Utilize the finite-element analytical method to generate the nonlinear force-deformation relationships among major components of a typical urban railcar.

Item 3: Develop the analytical methodology of passenger injury due to secondary collision to include modes of injury due to longitudinal, vertical, and pitching motions of the vehicles after impact. This methodology shall be capable of considering the location of the passenger prior to impact, his orientation (seated, standing, facing forward, facing sideways, facing rearward), the configuration of interior features of the cars, passengers density, and passenger restraint. This methodology shall also be capable of determining the severity of the injury sustained by the passenger.

Item 4: Utilize the results of Items 1 through 3 to develop guidelines for the evaluation of proposed railcar designs, and guidelines for the development of new railcars. These guidelines are to be developed in parametric form, so that individual parameters may be considered and the effects of specific values assigned or computed for these parameters may be assessed. These parameters are to include:

    a - the number of cars in the consist
    b - operational velocity ranges
    c - dimensions and weights of each car
    d - placement and dimensions of windows and doors
    e - placement and weights of mechanical/electrical
        equipment
    f - interior configurations of passenger compartment
    g - carbody force-deformation relationships among
        major structural subassemblages
    h - locations of carbody centers of gravity (c.g.).

## .1.2 Report Organization

This portion of the final report describes the work conducted under Items 2a and 2b. In order to meet the objectives of these tasks it was necessary to utilize the computer code described in Part 1 of this final report. The development of the consist model to be input to this code for the purpose of studying the primary collision of two impacting transit car consists is described in Section 2. In Section 3 the results of the computer runs using the consist models described in Section 2 are given. Procedures for generating the force-deformation relationships among major structural subassemblages of transit railcars is described in Section 4. A finite element technique is given in Subsection 4.1. This procedure is used in Subsections 4.1.1 and 4.1.2 to obtain the force-deformation relationships for the anticlimber and end sill structural subassembly and for the end of car superstructure subassembly of a typical urban transit car. In Subsection 4.2 testing techniques for obtaining force-deformation relationships are described. Subsection 4.2.1 gives a full-scale test procedure for obtaining the force-deformation relationships for the same two structural subassemblages investigated in Subsections 4.1.1 and 4.1.2. Finally scale model testing procedures are discussed in Section 4.2.2.

# 2. TRANSIT CAR CONSIST MODEL

Two separate computer models were developed for the simulation of the primary collision between two impacting consists of urban railcars. The initial model was considerably more complex than the second simplified model. Both models were run on the IITRAIN computer code for a 20 mph impact. The results of these runs are given in Section 3.

## 2.1 Initial Consist Model

Each of the consists modeled is composed of eight cars. One of these consists is assumed to be unloaded and moving at 20 mph at the time of impact. The second consist is assumed to be loaded, each car carrying approximately 31,000 lb of payload and standing motionless. The payload is assumed to be seated passengers equally distributed over the seating area of the car. Each of the consists is initially in a steady state condition with no braking or drive torque being applied. Except for the passenger loading and a slight misalignment of the anticlimbers, the two consists are otherwise assumed to be identical.

Each of the eight-car consists uses four different car models for the description of the total consist, as illustrated in Figure 1. The impacting, or impacted car is described by a nine-mass model; three masses for the coupler/drawbar; four masses for the sprung body; and one mass for each of the trucks. This is called car model Type A, as shown in Figure 2. Car model Type A is identical to the final transit car model used to assess the critical parameters of impact controlling devices during initial impact.

The second car uses a five-mass model, called car model Type B, also shown in Figure 2. Here the three-mass coupler/drawbar system is eliminated and replaced by a single drawbar element. The body is further simplified to a three-mass system, with the rest of the car system being the same as used in car model Type A. The third and fourth cars of the consist are each modeled as a three-mass system called car model Type C shown in Figure 3.

Impact Car



Car 1
Model Type A
Nine Mass

Car 2
Model Type B
Five Mass

Car 3
Model Type C
Three Mass

Car 4
Model Type C
Three Mass

Car 5
Model Type D
One Mass

Car 6
Model Type D
One Mass

Car 7
Model Type D
One Mass

Car 8
Model Type D
One Mass
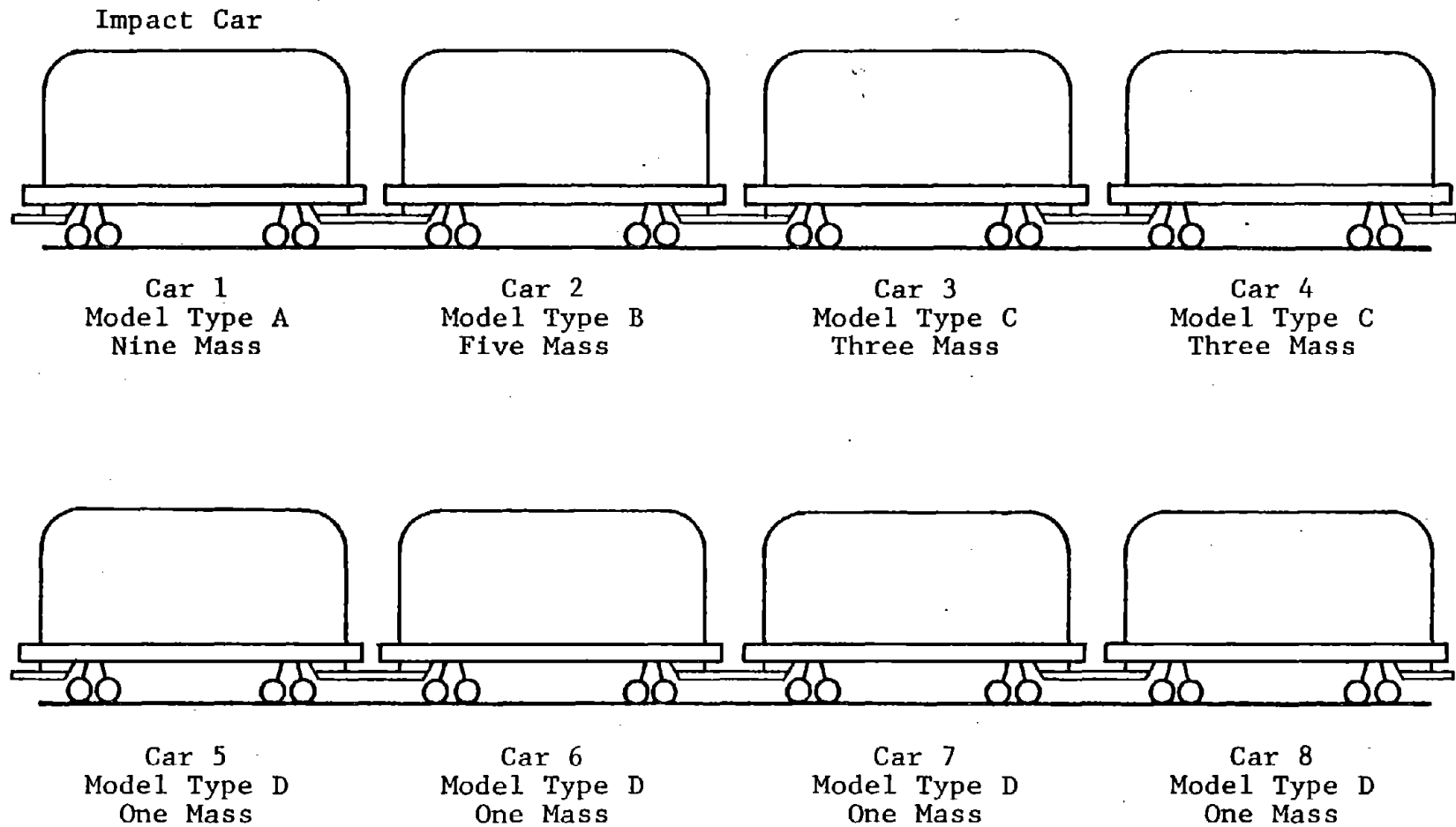
FIGURE 1.   EIGHT-CAR CONSIST MODEL

(Impact End)

Car 1
Model Type A
Nine Mass

Car 2
Model Type B
Five Mass
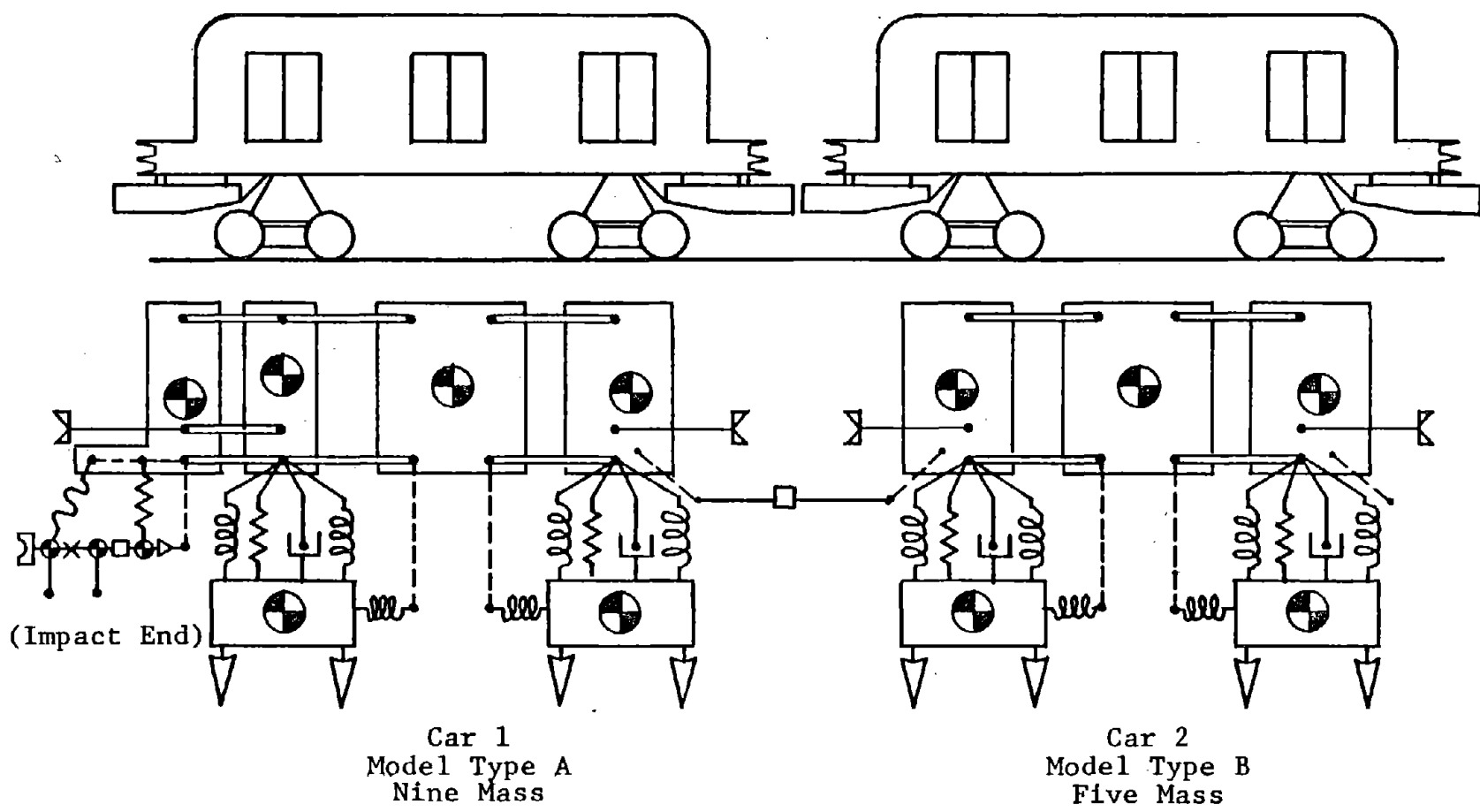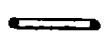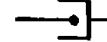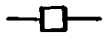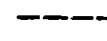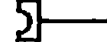
| | | | |
|---|---|---|---|
| ◁— | Wheel-Rail Interaction | ⬭ | Elastic-Plastic Beam |
| ⌁— | Linear Spring | ⊱— | Anticlimber |
| ⊷— | Nonlinear Spring | ▷— | Tapered Beam |
| —•⊦ | Nonlinear Dashpot | ⊟— | Draft Gear |
| ----- | Rigid Link | ⊁— | Pin Joint |
| ⋺— | Coupler End | ⋀— | Special Spring |

FIGURE 2.   CAR MODEL TYPES A AND B
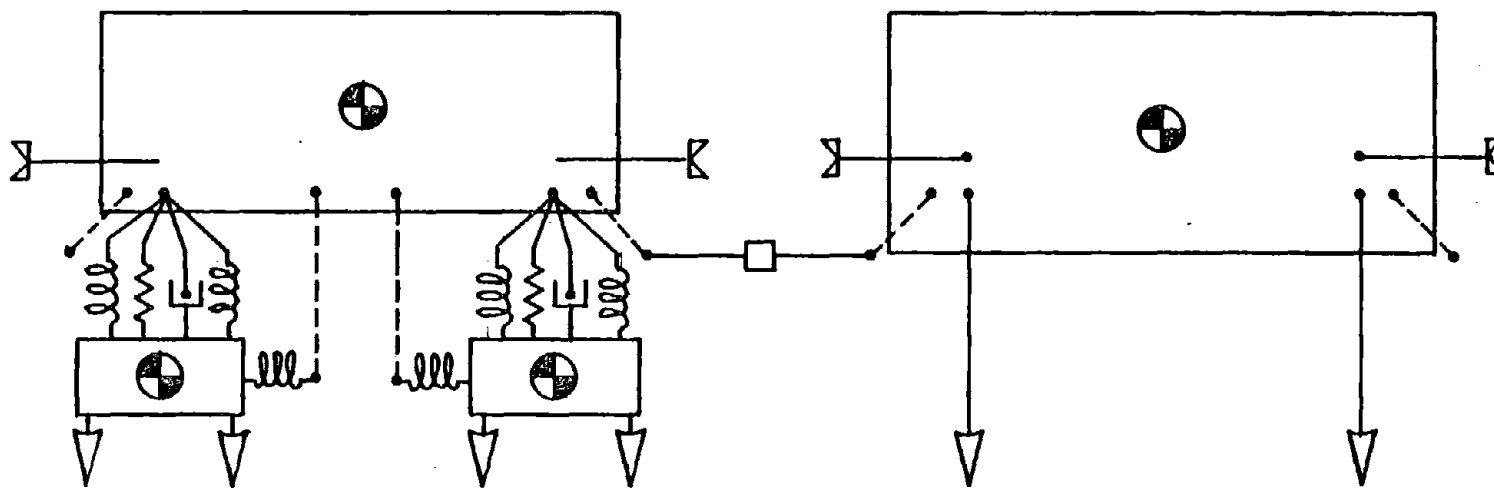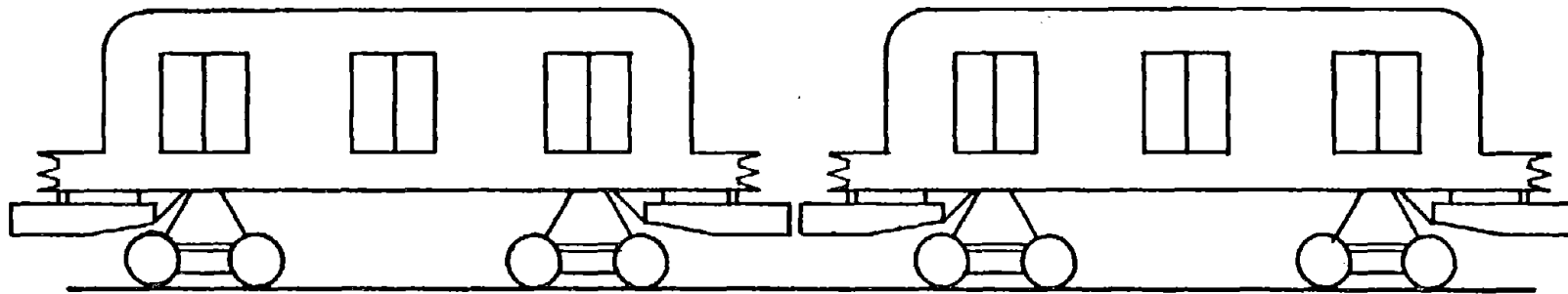
Cars 3 and 4
Model Type C
Three Mass

Cars 5, 6, 7 and 8
Model Type D
One Mass
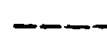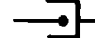
⊲— Wheel-Rail Interaction  ----- Rigid Links
-W\- Linear Spring  ⧽— Anticlimber
-lll- Nonlinear Spring  ⟋\⟍ Special Spring
—•|- Nonlinear Dashpot  -□- Draft Gear

FIGURE 3. CAR MODEL TYPES C AND D

8

The car body is assumed to be a single rigid mass, and each of the truck assemblies is still considered a separate mass. This allows complete pitch and vertical movement of the car body while reducing the total model complexity.

The final four cars of the consists are each considered as single mass systems. The crush characteristics of each car, and the coupling between cars remains unchanged. The wheel-rail interactions used in this car model are modified to allow approximately the same force deflection relationships of the car body as were previously allowed by the suspension. This single body model is called car model Type D, also illustrated in Figure 3.

The physical data describing each of the car models are derived from the data compiled for the most intricate model. Table 1 gives the weights and inertia properties of the various masses comprising the two consists. The locations of the attachment points relative to the mass c.g. for the element interconnecting the masses of the unloaded consist are listed in Table 2. The attachment points for the loaded consist are identical to those for the unloaded consist, with adjustments made for the change in the position of the c.g. due to the added load. The physical properties of the interconnecting elements used to characterize the model are listed in Table 3. The suspension properties for the loaded cars differ slightly to allow for the additional preload required and the change in stiffness.

## 2.2 Simplified Consist Model

The models for each of the two eight-car consists were further simplified to determine the sensitivity of the simulation results to the intricacy of the consist model. The cars of the consists were modeled as a single-mass system, each of which maintains the full crush characterization of the anticlimber. The cars are connected by a single drawbar element which represents the coupler/drawbar system. Two wheel-rail interaction elements are used on each car.

9

TABLE 1.-TRANSIT CONSIST MODEL MASS DATA

| Description | Mass | Weight (lb) | Inertia $(lb\text{-}sec^2\text{-}inch)$ | Global* X-position (inch) | Global* Y-position (inch) |
|---|---|---|---|---|---|
| **Unloaded Consist** | | | | | |
| ● Car 1 - Impacting Car | | | | | |
| Coupler end mass | 1 | 75 | 60 | 8.35 | 31.60 |
| Draft gear yoke mass | 2 | 90 | 70 | 25.40 | 31.60 |
| Draft gear housing mass | 3 | 150 | 100 | 40.00 | 31.60 |
| Front car end mass | 4 | 5,595 | 3,000 | 42.50 | 58.40 |
| Front mass over body bolster | 5 | 2,230 | 2,000 | 109.88 | 80.00 |
| Front truck assembly mass | 6 | 12,700 | 44,200 | 110.51 | 18.00 |
| Center body mass | 7 | 20,350 | 1,158,100 | 415.88 | 66.80 |
| Rear body mass | 8 | 7,825 | 29,750 | 775.06 | 64.60 |
| Rear truck assembly mass | 9 | 12,700 | 44,200 | 721.25 | 18.00 |
| ● Car 2 | | | | | |
| Front body mass | 10 | 7,825 | 29,750 | 888.44 | 64.56 |
| Front truck assembly mass | 11 | 12,700 | 44,200 | 942.26 | 18.00 |
| Center body mass | 12 | 20,350 | 1,158,100 | 1247.63 | 66.80 |
| Rear body mass | 13 | 7,825 | 29,750 | 1606.81 | 64.56 |
| Rear truck assembly mass | 14 | 12,700 | 44,200 | 1553.00 | 18.00 |
| ● Car 3 | | | | | |
| Body mass | 15 | 36,000 | 6,437,550 | 2079.38 | 65,83 |
| Front truck assembly mass | 16 | 12,700 | 44,200 | 1774.01 | 18.00 |
| Rear truck assembly mass | 17 | 12,700 | 44,200 | 2384.75 | 18.00 |
| ● Car 4 | | | | | |
| Body mass | 18 | 36,000 | 6,437,550 | 2911.13 | 65.83 |
| Front truck assembly mass | 19 | 12,700 | 44,200 | 2605.76 | 18.00 |
| Rear truck assembly mass | 20 | 12,700 | 44,200 | 3216.50 | 18.00 |
| ● Car 5 | | | | | |
| Total car mass | 21 | 61,400 | 7,310,826 | 3742.88 | 46.04 |
| ● Car 6 | | | | | |
| Total car mass | 22 | 61,400 | 7,310,826 | 4574.63 | 46.04 |

*Global positions are measured from rail level and from the initial position of the impacting coupler faces.

10

TABLE 1.-TRANSIT CONSIST MODEL MASS DATA (Contd)

| Description | Mass | Weight (lb) | Inertia $(lb-sec^2-inch)$ | Global* X-position (inch) | Global* Y-position (inch) |
|---|---|---|---|---|---|
| ● Car 7 | | | | | |
| Total car mass | 23 | 61,400 | 7,310,826 | 5406.38 | 46.04 |
| ● Car 8 - Trailing Car | | | | | |
| Total car mass | 24 | 61,400 | 7,310,826 | 6238.13 | 46.04 |
| Loaded Consist | | | | | |
| ● Car 1 - Impacted Car | | | | | |
| Coupler end mass | 25 | 75 | 60 | -8.35 | 31.60 |
| Draft gear yoke mass | 26 | 90 | 70 | -25.40 | 31.60 |
| Draft gear housing mass | 27 | 150 | 100 | -40.00 | 31.60 |
| Front car end mass | 28 | 6,180 | 4,000 | -44.25 | 59.67 |
| Front mass over body bolster | 29 | 3,230 | 3,000 | -109.88 | 77.48 |
| Front truck assembly mass | 30 | 12,700 | 44,200 | -110.51 | 18.00 |
| Center body mass | 31 | 47,923 | 253,200 | -415.88 | 69.71 |
| Rear body mass | 32 | 9,408 | 35,000 | -773.50 | 65.79 |
| Rear truck assembly mass | 33 | 12,700 | 44,200 | -721.25 | 18.00 |
| ● Car 2 | | | | | |
| Front body mass | 34 | 9,408 | 35,000 | -890.00 | 65.79 |
| Front truck assembly mass | 35 | 12,700 | 44,200 | -942.26 | 18.00 |
| Center body mass | 36 | 47,923 | 2,532,000 | -1247.63 | 69.71 |
| Rear body mass | 37 | 9,408 | 35,000 | -1605.25 | 65.79 |
| Rear truck assembly mass | 38 | 12,700 | 44,200 | -1553.00 | 18.00 |
| ● Car 3 | | | | | |
| Body mass | 39 | 66,739 | 8,856,844 | -2079.38 | 68.60 |
| Front truck assembly mass | 40 | 12,700 | 44,200 | -1774.01 | 18.00 |
| Rear truck assembly mass | 41 | 12,700 | 44,200 | -2384.75 | 18.00 |
| ● Car 4 | | | | | |
| Body mass | 42 | 66,739 | 8,856,844 | -2911.13 | 68.60 |
| Front truck assembly mass | 43 | 12,700 | 44,200 | -2605.76 | 18.00 |
| Rear truck assembly mass | 44 | 12,700 | 44,200 | -3216.50 | 18.00 |

TABLE 1.-TRANSIT CONSIST MODEL MASS DATA (Concl)

| Description | Mass | Weight (lb) | Inertia (lb-sec$^2$-inch) | Global* X-position (inch) | Global* Y-position (inch) |
|---|---|---|---|---|---|
| • Car 5 | | | | | |
| Total car mass | 45 | 92,139 | 12,009,653 | -3742.88 | 39.03 |
| • Car 6 | | | | | |
| Total car mass | 46 | 92,139 | 12,009,653 | -4574.63 | 39.03 |
| • Car 7 | | | | | |
| Total car mass | 47 | 92,139 | 12,009,653 | -5406.38 | 39.03 |
| • Car 8 | | | | | |
| Total car mass | 48 | 92,139 | 12,009,653 | -6238.13 | 39.03 |

TABLE 2.—CONNECTION POINT DATA

| Connection Description | Element | Local* X-Position (inch) | Local* Y-Position (inch) |
|---|---|---|---|
| ● Mass 1 - Coupler End Mass - Car 1 | | | |
| Coupling between coupler faces | Coupler end | -7.35 | 0.00 |
| Pin between coupler end and draft gear yoke | Pin joint | 8.70 | 0.00 |
| Coupler leveler spring | Special spring (Type 1) | 8.15 | -6.30 |
| Interference between coupler end and underside of end sill | Special spring (Type 2) | -8.00 | 5.80 |
| ● Mass 2 - Draft Gear Yoke Mass - Car 1 | | | |
| Pin between coupler end and draft gear yoke | Pin joint | -8.35 | 0.00 |
| Coupler leveler spring | Special spring (Type 1) | -7.65 | -6.30 |
| Draft gear connection | Draft gear (Type 1) slider joint | 0.00 0.00 | 0.00 0.00 |
| ● Mass 3 - Draft Gear Housing Mass - Car 1 | | | |
| Draft gear connection | Draft gear (Type 1) slider joint | 0.00 0.00 | 0.00 0.00 |
| Rail slider connection to end sill | Nonlinear spring (Type 1) | -18.00 | 5.30 |
| Drawbar and draft pocket assembly connection to car body | Tapered beam | 0.00 | 0.00 |
| ● Mass 4 - Front Car End Mass - Car 1 | | | |
| Drawbar and draft pocket assembly connection to car body | Tapered beam | 17.5 | -26.80 |
| Rail slider connection to end sill | Nonlinear spring (Type 1) | -20.50 | -18.50 |
| Interference between coupler end and underside of end sill | Special spring (Type 2) | -40.60 | -10.40 |
| End sill/anticlimber | Anticlimber | 17.50 | -11.90 |
| Roof sill beam | Beam (Type 1) | 0.00 | 86.60 |
| Side sill beam | Beam (Type 2) | 0.00 | -14.80 |
| Draft sill beam | Beam (Type 3) | 17.50 | -14.80 |
| ● Mass 5 - Front Mass over Body Bolster - Car 1 | | | |
| Roof sill beam | Beam (Type 1) | 0.00 | 65.00 |
| Side sill beam | Beam (Type 2) | 0.00 | -36.40 |
| Draft sill beam | Beam (Type 3) | 0.00 | -36.40 |
| Suspension attachment at bolster | Linear spring Nonlinear spring (Type 2) Nonlinear spring (Type 3) Nonlinear dashpot | 0.00 | -34.00 |

*Local positions are measured from the mass center of gravity.

13

TABLE 2.-CONNECTION POINT DATA (Contd)

| Connection Description | Element | Local* X-Position (inch) | Local* Y-Position (inch) |
|---|---|---|---|
| **● Mass 6 - Front Truck Assembly Mass - Car 1** | | | |
| Suspension attachment at bolster | Linear spring<br>Nonlinear spring (Type 2)<br>Nonlinear spring (Type 3)<br>Nonlinear dashpot | -0.63 | 12.75 |
| Truck anchor connection | Nonlinear spring (Type 4) | 20.37 | 0.00 |
| Front wheel-rail interaction | Wheel-rail (Type 1) | -41.63 | -4.00 |
| Rear wheel-rail interaction | Wheel-rail (Type 1) | 40.37 | -4.00 |
| **● Mass 7 - Center Body Mass - Car 1** | | | |
| Roof sill beam | Beam (Type 1) | 0.00 | 78.20 |
| Side sill beam | Beam (Type 2) | 0.00 | -23.20 |
| Front truck anchor connection | Nonlinear spring (Type 4) | -252.00 | -48.80 |
| Rear truck anchor connection | Nonlinear spring (Type 4) | 252.00 | -48.80 |
| **● Mass 8 - Rear Body Mass - Car 1** | | | |
| Roof sill beam | Beam (Type 1) | 0.00 | 80.44 |
| Side sill beam | Beam (Type 2) | 0.00 | -20.96 |
| Suspension attachment at bolster | Linear spring<br>Nonlinear spring (Type 2)<br>Nonlinear spring (Type 3)<br>Nonlinear dashpot | -53.18 | -18.56 |
| Drawbar connection to second car | Draft gear (Type 2) | -3.30 | -32.96 |
| End sill/anticlimber | Anticlimber | -3.30 | -19.56 |
| **● Mass 9 - Rear Truck Assembly Mass - Car 1** | | | |
| Suspension attachment at bolster | Linear spring<br>Nonlinear spring (Type 2)<br>Nonlinear spring (Type 3)<br>Nonlinear dashpot | 0.63 | 12.75 |
| Truck anchor connection | Nonlinear spring (Type 4) | -20.37 | 0.00 |
| Front wheel-rail interaction | Wheel-rail (Type 1) | -40.37 | -4.00 |
| Rear wheel-rail interaction | Wheel-rail (Type 1) | 41.63 | -4.00 |
| **● Mass 10 - Front Body Mass - Car 2** | | | |
| Drawbar connection to first car | Draft gear (Type 2) | 3.30 | -32.96 |
| End sill/anticlimber | Anticlimber | 3.30 | -19.56 |
| Roof sill beam | Beam (Type 1) | 0.00 | 80.44 |
| Side sill beam | Beam (Type 2) | 0.00 | -20.96 |
| Suspension attachment at bolster | Linear spring<br>Nonlinear spring (Type 2)<br>Nonlinear spring (Type 3)<br>Nonlinear dashpot | 53.18 | -18.56 |

TABLE 2.–CONNECTION POINT DATA (Contd)

| Connection Description | Element | Local* X-Position (inch) | Local* Y-Position (inch) |
|---|---|---|---|
| ● Mass 11 - Front Truck Assembly Mass - Car 2 | | | |
| Suspension attachment at bolster | Linear spring<br>Nonlinear spring (Type 2)<br>Nonlinear spring (Type 3)<br>Nonlinear dashpot | -0.63 | 12.75 |
| Truck anchor connection | Nonlinear spring (Type 4) | 20.37 | 0.00 |
| Front wheel-rail interaction | Wheel-rail (Type 1) | -41.63 | -4.00 |
| Rear wheel-rail interaction | Wheel-rail (Type 1) | 40.37 | -4.00 |
| ● Mass 12 - Center Body Mass - Car 2 | | | |
| Roof sill beam | Beam (Type 1) | 0.00 | 78.20 |
| Side sill beam | Beam (Type 2) | 0.00 | -23.20 |
| Front truck anchor connection | Nonlinear spring (Type 4) | -252.00 | -48.80 |
| Rear truck anchor connection | Nonlinear spring (Type 4) | 252.00 | -48.80 |
| ● Mass 13 - Rear Body Mass - Car 2 | | | |
| Roof sill beam | Beam (Type 1) | 0.00 | 80.44 |
| Side sill beam | Beam (Type 2) | 0.00 | -20.96 |
| Suspension attachment at bolster | Linear spring<br>Nonlinear spring (Type 2)<br>Nonlinear spring (Type 3)<br>Nonlinear dashpot | -53.18 | -18.56 |
| Drawbar connection to third car | Draft gear (Type 2) | -3.30 | -32.96 |
| End sill/anticlimber | Anticlimber | -3.30 | -19.56 |
| ● Mass 14 - Rear Truck Assembly Mass - Car 2 | | | |
| Suspension attachment at bolster | Linear spring<br>Nonlinear spring (Type 2)<br>Nonlinear spring (Type 3)<br>Nonlinear dashpot | 0.63 | 12.75 |
| Truck anchor connection | Nonlinear spring (Type 4) | -20.37 | 0.00 |
| Front wheel-rail interaction | Wheel-rail (Type 1) | -40.37 | -4.00 |
| Rear wheel-rail interaction | Wheel-rail (Type 1) | 41.63 | -4.00 |
| ● Mass 15 - Body Mass - Car 3 | | | |
| Drawbar connection to second car | Draft gear (Type 2) | -355.90 | -34.23 |
| Drawbar connection to fourth car | Draft gear (Type 2) | 355.90 | -34.23 |
| Front end sill/anticlimber | Anticlimber | -355.90 | -20.83 |
| Rear end sill/anticlimber | Anticlimber | 355.90 | -20.83 |
| Front suspension attachment at bolster | Linear spring<br>Nonlinear spring (Type 2)<br>Nonlinear spring (Type 3)<br>Nonlinear dashpot | -306.00 | -19.83 |

TABLE 2.-CONNECTION POINT DATA (Contd)

| Connection Description | Element | Local* X-Position (inch) | Local* Y-Position (inch) |
|---|---|---|---|
| ● Mass 15 (Concl) | | | |
| Rear suspension attachment at bolster | Linear spring Nonlinear spring (Type 2) Nonlinear spring (Type 3) Nonlinear dashpot | 306.00 | -19.83 |
| Front truck anchor connection | Nonlinear spring (Type 4) | -252.00 | -47.83 |
| Rear truck anchor connection | Nonlinear spring (Type 4) | 252.00 | -47.83 |
| ● Mass 16 - Front Truck Assembly Mass - Car 3 | | | |
| Suspension attachment at bolster | Linear spring Nonlinear spring (Type 2) Nonlinear spring (Type 3) Nonlinear dashpot | -0.63 | 12.75 |
| Truck anchor connection | Nonlinear spring (Type 4) | 20.37 | 0.00 |
| Front wheel-rail interaction | Wheel-rail (Type 1) | -41.63 | -4.00 |
| Rear wheel-rail interaction | Wheel-rail (Type 1) | 40.37 | -4.00 |
| ● Mass 17 - Rear Truck Assembly Mass - Car 3 | | | |
| Suspension attachment at bolster | Linear spring Nonlinear spring (Type 2) Nonlinear spring (Type 3) Nonlinear dashpot | 0.63 | 12.75 |
| Truck anchor connection | Nonlinear spring (Type 4) | -20.37 | 0.00 |
| Front wheel-rail interaction | Wheel-rail (Type 1) | -40.37 | -4.00 |
| Rear wheel-rail interaction | Wheel-rail (Type 1) | 41.63 | -4.00 |
| ● Mass 18 - Body Mass - Car 4 | | | |
| Drawbar connection to third car | Draft gear (Type 2) | -355.90 | -34.23 |
| Drawbar connection to fifth car | Draft gear (Type 2) | 355.90 | -34.23 |
| Front end sill/anticlimber | Anticlimber | -355.90 | -20.83 |
| Rear end sill/anticlimber | Anticlimber | 355.90 | -20.83 |
| Front suspension attachment at bolster | Linear spring Nonlinear spring (Type 2) Nonlinear spring (Type 3) Nonlinear dashpot | -306.00 | -19.83 |
| Rear suspension attachment at bolster | Linear spring Nonlinear spring (Type 2) Nonlinear spring (Type 3) Nonlinear dashpot | 306.00 | -19.83 |
| Front truck anchor connection | Nonlinear spring (Type 4) | -252.00 | -47.83 |
| Rear truck anchor connection | Nonlinear spring (Type 4) | 252.00 | -47.83 |

TABLE 2.-CONNECTION POINT DATA (Contd)

| Connection Description | Element | Local* X-Position (inch) | Local* Y-Position (inch) |
|---|---|---|---|
| ● Mass 19 - Front Truck Assembly Mass - Car 4 | | | |
| Suspension attachment at bolster | Linear spring<br>Nonlinear spring (Type 2)<br>Nonlinear spring (Type 3)<br>Nonlinear dashpot | -0.63 | 12.75 |
| Truck anchor connection | Nonlinear spring (Type 4) | 20.37 | 0.00 |
| Front wheel-rail interaction | Wheel-rail (Type 1) | -41.63 | -4.00 |
| Rear wheel-rail interaction | Wheel-rail (Type 1) | 40.37 | -4.00 |
| ● Mass 20 - Rear Truck Assembly Mass - Car 4 | | | |
| Suspension attachment at bolster | Linear spring<br>Nonlinear spring (Type 2)<br>Nonlinear spring (Type 3)<br>Nonlinear dashpot | 0.63 | 12.75 |
| Truck anchor connection | Nonlinear spring (Type 4) | -20.37 | 0.00 |
| Front wheel-rail interaction | Wheel-rail (Type 1) | -40.37 | -4.00 |
| Rear wheel-rail interaction | Wheel-rail (Type 1) | 41.63 | -4.00 |
| ● Mass 21 - Total Car Mass - Car 5 | | | |
| Drawbar connection to fourth car | Draft gear (Type 2) | -355.90 | -14.44 |
| Drawbar connection to sixth car | Draft gear (Type 2) | 355.90 | -14.44 |
| Front end sill/anticlimber | Anticlimber | -355.90 | -1.04 |
| Rear end sill/anticlimber | Anticlimber | 355.90 | -1.04 |
| Front wheel-rail interaction | Wheel-rail (Type 2) | -306.00 | -32.04 |
| Rear Wheel-rail interaction | Wheel-rail (Type 2) | 306.00 | -32.04 |
| ● Mass 22 - Total Car Mass - Car 6 | | | |
| Drawbar connection to fifth car | Draft gear (Type 2) | -355.90 | -14.44 |
| Drawbar connection to seventh car | Draft gear (Type 2) | 355.90 | -14.44 |
| Front end sill/anticlimber | Anticlimber | -355.90 | -1.04 |
| Rear end sill/anticlimber | Anticlimber | 355.90 | -1.04 |
| Front wheel-rail interaction | Wheel-rail (Type 2) | -306.00 | -32.04 |
| Rear Wheel-rail interaction | Wheel-rail (Type 2) | 306.00 | -32.04 |
| ● Mass 23 - Total Car Mass - Car 7 | | | |
| Drawbar connection to sixth car | Draft gear (Type 2) | -355.90 | -14.44 |
| Drawbar connection to eighth car | Draft gear (Type 2) | 355.90 | -14.44 |
| Front end sill/anticlimber | Anticlimber | -355.90 | -1.04 |
| Rear end sill/anticlimber | Anticlimber | 355.90 | -1.04 |
| Front wheel-rail interaction | Wheel-rail (Type 2) | -306.00 | -32.04 |
| Rear Wheel-rail interaction | Wheel-rail (Type 2) | 306.00 | -32.04 |

TABLE 2.-CONNECTION POINT DATA (Concl)

| Connection Description | Element | Local* X-Position (inch) | Local* Y-Position (inch) |
|---|---|---|---|
| • Mass 24 - Total Car Mass - Car 8 | | | |
| Drawbar connection to seventh car | Draft gear (Type 2) | -355.90 | -14.44 |
| Front end sill/anticlimber | Anticlimber | -355.90 | -1.04 |
| Rear end sill/anticlimber | Anticlimber | 355.90 | -1.04 |
| Front wheel-rail interaction | Wheel-rail (Type 2) | -306.00 | -32.04 |
| Rear wheel-rail interaction | Wheel-rail (Type 2) | 306.00 | -32.04 |

## TABLE 3.–PHYSICAL PROPERTIES OF ELEMENTS

### Coupler End

| | | | |
|---|---|---|---|
| Horizontal stiffness, end K | = 360,000 lb/inch | Horizontal stiffness, end $\ell$ | = 360,000 lb/inch |
| Free length, end K | = 1 inch | Free length, end $\ell$ | = 1 inch |
| Coupler height, end K | = 12 inches | Coupler height, end $\ell$ | = 12 inches |
| Total horizontal slack | = 0.0 inch | | |

### Pin Joint

Friction parameter ($\mu$R) = 0.3

### Special Spring (Type 1)

| | | | |
|---|---|---|---|
| Compressive stiffness, compression < $\delta_c$ | = 5000 lb/inch | Preload | = 1250 lb |
| Compressive stiffness, compression > $\delta_c$ | = 3,000,000 lb/inch | Fracture load | = 400,000 lb |
| $\delta_c$ | = 1.25 inch | Free length | = 1.25 inch |

### Special Spring (Type 2)

| | | | |
|---|---|---|---|
| Compressive stiffness, compression < $\delta_c$ | = 0.0 lb/inch | Preload | = 0.0 lb |
| Compressive stiffness, compression > $\delta_c$ | = 175,000 lb/inch | Fracture load | = 700,000 lb |
| $\delta_c$ | = 4.0 inches | Free length | = 4.0 inches |

### Draft Gear (Type 1)

| | | | |
|---|---|---|---|
| Initial stiffness | = 24,000 lb/inch | Hysteresis load | = 10,000 lb |
| Travel | = 1.25 inch | Pin shear load | = 150,000 lb |
| Stiffness after bottoming | = 320,000 lb/inch | Postshear travel | = 1.375 inch |
| | | Fracture load | = 250,000 lb |

### Draft Gear (Type 2)

| | | | |
|---|---|---|---|
| Initial stiffness | = 12,000 lb/inch | Hysteresis load | = 10,000 lb |
| Travel | = 2.50 inch | Pin shear load | = 150,000 lb |
| Stiffness after bottoming | = 160,000 lb/inch | Postshear travel | = 10.0 inches |
| | | Fracture load | = 250,000 lb |

## TABLE 3.-PHYSICAL PROPERTIES OF ELEMENTS (Contd)

### Tapered Beam

| | | | |
|---|---|---|---|
| Elastic modulus | $= 3 \times 10^{7}$ psi | Height, end K | = 3.273 inches |
| Plastic modulus | = 180,000 psi | Width, end K | = 2.830 inches |
| Yield stress | = 100,000 psi | Height, end $\ell$ | = 5.475 inches |
| Ultimate stress | = 200,000 psi | Width, end $\ell$ | = 1.827 inch |

### Anticlimber

| | | | |
|---|---|---|---|
| Vertical elastic stiffness, end K | = 175,000 lb/inch | Vertical elastic stiffness, end $\ell$ | = 175,000 lb/inch |
| Vertical plastic stiffness, end K | = 1633 lb/inch | Vertical plastic stiffness, end $\ell$ | = 1633 lb/inch |
| Vertical yield deflection, end K | = 0.20 inch | Vertical yield deflection, end $\ell$ | = 0.20 inch |
| Vertical rupture deflection, end K | = 5 inches | Vertical rupture deflection, end $\ell$ | = 5 inches |
| Horizontal elastic stiffness, end K | = 4,450,000 lb/inch | Horizontal elastic stiffness, end $\ell$ | = 4,450,000 lb/inch |
| Horizontal plastic stiffness, end K | = 20,620 lb/inch | Horizontal plastic stiffness, end $\ell$ | = 20,620 lb/inch |
| Horizontal yield defleciton, end K | = 0.053 inch | Horizontal yield deflection, end $\ell$ | = 0.053 inch |
| Horizontal rupture deflection, end K | = 56 inches | Horizontal rupture deflection, end $\ell$ | = 56 inches |
| Torsional elastic stiffness, end K | = 110,800 inch-lb/rad | Torsional elastic stiffness, end $\ell$ | = 110,800 inch-lb/rad |
| Torsional plastic stiffness, end K | = 25,500 inch-lb/rad | Torsional plastic stiffness, end $\ell$ | = 25,500 inch-lb/rad |
| Torsional yield deflection, end K | = 0.001 rad | Torsional yield deflection, end $\ell$ | = 0.001 rad |
| Torsional rupture deflection, end K | = 1 rad | Torsional rupture deflection, end $\ell$ | = 1 rad |
| Face height, end K | = 6 inches | Face height, end $\ell$ | = 6 inches |
| Length, end K | = 58.125 inches | Length, end $\ell$ | = 58.125 inches |

TABLE 3.-PHYSICAL PROPERTIES OF ELEMENTS (Contd)

Beam (Type 1)

| | | | |
|---|---|---|---|
| Elastic modulus | $= 1 \times 10^7$ psi | Ultimate stress | = 100,000 psi |
| Plastic modulus | = 20,000 psi | Height | = 19.55 inches |
| Yield stress | = 60,000 psi | Width | = 0.676 inch |

Beam (Type 2)

| | | | |
|---|---|---|---|
| Elastic modulus | $= 1 \times 10^7$ psi | Ultimate stress | = 100,000 psi |
| Plastic modulus | = 20,000 psi | Height | = 9.790 inches |
| Yield stress | = 60,000 psi | Width | = 2.082 inches |

Beam (Type 3)

| | | | |
|---|---|---|---|
| Elastic modulus | $= 3 \times 10^7$ psi | Ultimate stress | = 150,000 psi |
| Plastic modulus | = 180,000 psi | Height | = 10.360 inches |
| Yield stress | = 100,000 psi | Width | = 0.776 inch |

Linear Spring * Adjusted for Load

| | | | |
|---|---|---|---|
| Spring constant | = 3110 lb/inch | Free length | = 20.04 inches |

Nonlinear Spring (Type 1)

| | | | |
|---|---|---|---|
| Compressive constant, Compression $< \delta_c$ | $= 3 \times 10^6$ lb/inch | Extension constant, extension $< \delta_t$ | = 75,000 lb/inch |
| Compressive constant, compression $> \delta_c$ | $= 3 \times 10^6$ lb/inch | Extension constant, extension $> \delta_t$ | = 75,000 lb/inch |
| $\delta_c$ | = 10 inches | $\delta_t$ | = 10 inches |
| Free length | = 3 inches | | |

Nonlinear Spring (Type 2)

| | | | |
|---|---|---|---|
| Compressive constant, compression $< \delta_c$ | = 0.0 lb/inch | Extension constant, extension $< \delta_t$ | = 0.0 lb/inch |
| Compressive constant, compression $> \delta_c$ | $= 3 \times 10^6$ lb/inch | Extension constant, extension $> \delta_t$ | $= 3 \times 10^6$ lb/inch |
| $\delta_c$ | = 3.75 inches | $\delta_t$ | = 2 inches |
| Free length | = 14.25 inches | | |

## TABLE 3.-PHYSICAL PROPERTIES OF ELEMENTS (Contd)

### Nonlinear Spring (Type 3)* Adjusted for Load

| | | | |
|---|---|---|---|
| Compressive constant, compression < $\delta_c$ | = 0.0 lb/inch | Extension constant, extension < $\delta_t$ | = 0.0 lb/inch |
| Compressive constant, compression > $\delta_c$ | = 26,890 lb/inch | Extension constant, extension > $\delta_t$ | = 0.0 lb/inch |
| $\delta_c$ | = 2.79 inches | $\delta_t$ | = 1 inch |
| Free length | = 14.25 inches | | |

### Nonlinear Spring (Type 4)

| | | | |
|---|---|---|---|
| Compressive constant, compression < $\delta_c$ | = 500,000 lb/inch | Extension constant, extension < $\delta_t$ | = 500,000 lb/inch |
| Compressive constant, compression > $\delta_c$ | = 4,500,000 lb/inch | Extension constant, extension > $\delta_t$ | = 4,500,000 lb/inch |
| $\delta_c$ | = 0.625 inch | $\delta_t$ | = 0.625 inch |
| Free length | = 33 inches | | |

### Nonlinear Dashpot

| | | | |
|---|---|---|---|
| Damping constant compression, velocity < $V_c$ | = 1180 lb-sec/inch | Damping constant extension, velocity < $V_t$ | = 1180 lb-sec/inch |
| Damping constant compression, velocity > $V_c$ | = 173 lb-sec/inch | Damping constant extension, velocity > $V_t$ | = 173 lb-sec/inch |
| $V_c$ | = 4.5 inch/sec | $V_t$ | = 4.5 inch/sec |

### Slider Joint

| | | | |
|---|---|---|---|
| Slider length | = 10 inches | Coefficient of friction | = 0.01 |
| Slider width | = 1 inch | | |

## TABLE 3.-PHYSICAL PROPERTIES OF ELEMENTS (Concl)

Wheel-Rail (Type 1)

| | | | |
|---|---|---|---|
| Spring constant deflection < $\delta_L$ | = 3,234,000 lb/inch | Wheel radius | = 14 inches |
| Spring constant deflection > $\delta_L$ | = 3,234,000 lb/inch | Damping constant | = 1000 lb-sec/inch |
| $\delta_L$ | = 5 inches | | |

Wheel-Rail (Type 2) * Adjusted for Load

| | | | |
|---|---|---|---|
| Spring constant deflection < $\delta_L$ | = 6,468,000 lb/inch | Wheel radius | = 14 inches |
| Spring constant deflection > $\delta_L$ | = 6,468,000 lb/inch | Damping constant | = 1000 lb-sec/inch |
| $\delta_L$ | = 5 inches | | |

These elements are modeled to approximately yield a force deflection relationship which represents the motion of the suspension, trucks and wheel-rail interactions. This car model is illustrated in Figure 4.

The physical data describing the car models are derived from the data compiled for the more intricate models used previously. The weights and inertia properties of the masses comprising this model are listed in Table 4. The locations of the attachment points relative to the mass c.g. for the element interconnecting the masses of the consists are listed in Table 5. The attachment points for the loaded consist are identical to those for the unloaded consist, with adjustments made for the change in the position of the c.g. due to the added load. The physical properties of the interconnecting elements used to characterize the model are listed in Table 6. The suspension properties for the loaded cars differ slightly to allow for the additional preload required and the change in stiffness.
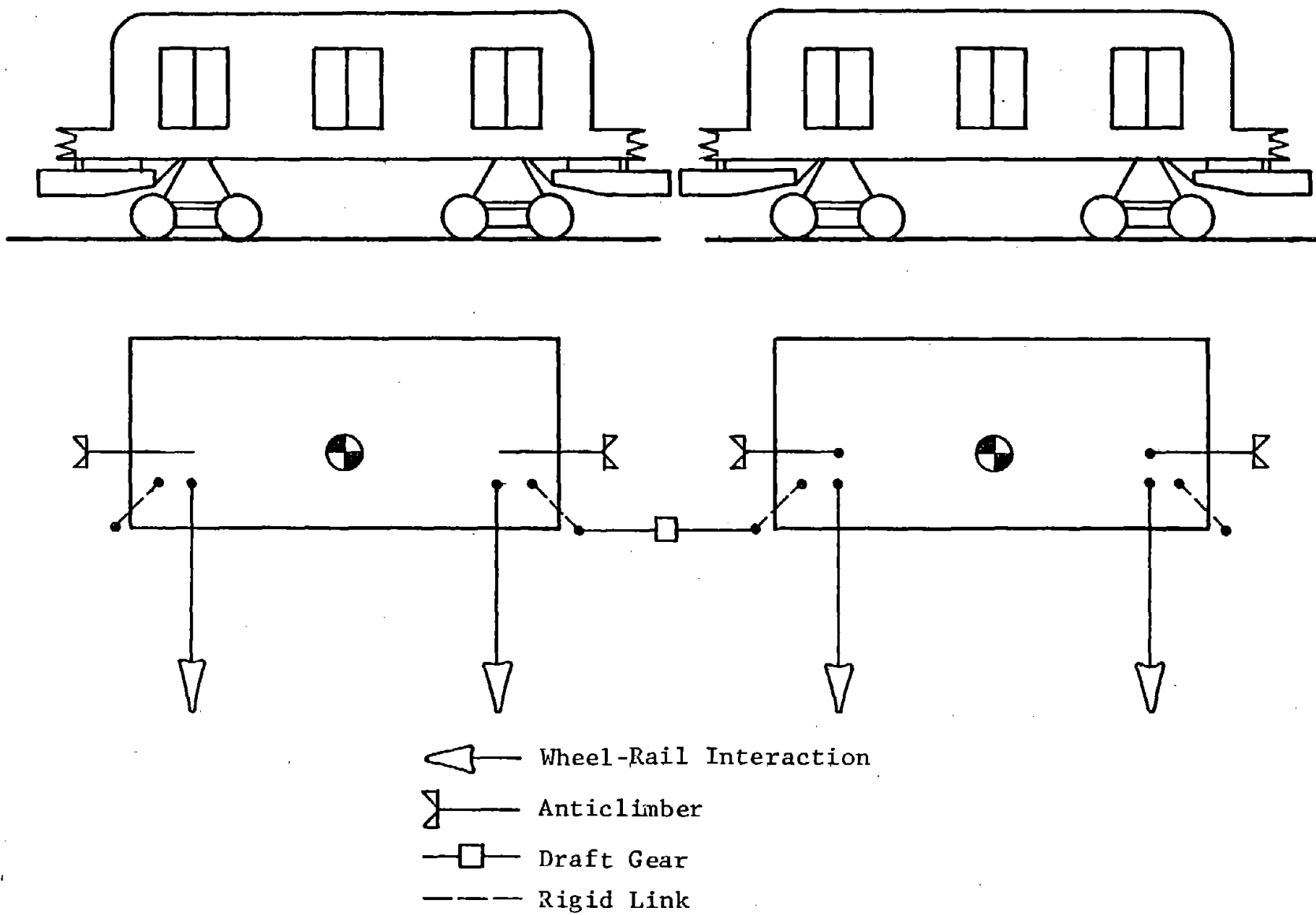
Wheel-Rail Interaction

Anticlimber

Draft Gear

Rigid Link

FIGURE 4.   SIMPLIFIED CONSIST MODEL

TABLE 4.–TRANSIT CONSIST MODEL MASS DATA

| Description | Weight (lb) | Inertia (lb-sec$^2$-inch) | Global* X-Position (inch) | Global* Y-Position (inch) |
|---|---|---|---|---|
| **Unloaded Consist** | | | | |
| Car 1 – Impacting Car | 61,400 | 7,310,826 | 415.875 | 46.04 |
| Car 2 | 61,400 | 7,310,826 | 1247.625 | 46.04 |
| Car 3 | 61,400 | 7,310,826 | 2079.375 | 46.04 |
| Car 4 | 61,400 | 7,310,826 | 2911.125 | 46.04 |
| Car 5 | 61,400 | 7,310,826 | 3742.875 | 46.04 |
| Car 6 | 61,400 | 7,310,826 | 4574/625 | 46.04 |
| Car 7 | 61,400 | 7,310,826 | 5406.375 | 46.04 |
| Car 8 | 61,400 | 7,310,826 | 6238.125 | 46.04 |
| **Loaded Consist** | | | | |
| Car 1 – Impacted Car | 92,139 | 12,009,653 | -415.875 | 39.03 |
| Car 2 | 92,139 | 12,009,653 | -1247.625 | 39.03 |
| Car 3 | 92,139 | 12,009,653 | -2079.375 | 39.03 |
| Car 4 | 92,139 | 12,009,653 | -2911.125 | 39.03 |
| Car 5 | 92,139 | 12,009,653 | -3742.875 | 39.03 |
| Car 6 | 92,139 | 12,009,653 | -4574.625 | 39.03 |
| Car 7 | 92,139 | 12,009,653 | -5406.375 | 39.03 |
| Car 8 | 92,139 | 12,009,653 | -6238.125 | 39.03 |

*Global positions are measured from rail level and from the initial position of the impacting coupler faces.

TABLE 5.-CONNECTION POINT DATA

| Connection Description | Element | Local* X-Position (inch) | Local* Y-Position (inch) |
|---|---|---|---|
| **Unloaded Consist** | | | |
| ● Car 1 - Impacting Car | | | |
| Drawbar connection to car in front | Draft gear (Type 1) | -306.0 | -32.04 |
| Drawbar connection to car in rear | Draft gear (Type 2) | 306.0 | -32.04 |
| Front end sill/anticlimber | Anticlimber | -355.9 | 0.46 |
| Rear end sill/anticlimber | Anticlimber | 355.9 | -1.04 |
| Front wheel-rail interaction | Wheel-rail | -355.9 | -14.44 |
| Rear wheel-rail interaction | Wheel-rail | 355.9 | -14.44 |
| ● Car 2 | | | |
| Drawbar connection to car in front | Draft gear (Type2) | -306.0 | -32.04 |
| Drawbar connection to car in rear | Draft gear (Type 1) | 306.0 | -32.04 |
| Front end sill/anticlimber | Anticlimber | -355.9 | 0.46 |
| Rear end sill/anticlimber | Anticlimber | 355.9 | -1.04 |
| Front wheel-rail interaction | Wheel-rail | -355.9 | -14.44 |
| Rear wheel rail interaction | Wheel-rail | 355.9 | -14.44 |
| **Loaded Consist** | | | |
| ● Car 1 - Impacted Car | | | |
| Drawbar connection to car in front | Draft gear (Type 1) | 306.0 | -25.03 |
| Drawbar connection to car in rear | Draft gear (Type 2) | -306.0 | -25.03 |
| Front end sill/anticlimber | Anticlimber | 355.9 | 5.97 |
| Rear end sill/anticlimber | Anticlimber | -355.9 | 7.47 |
| Front wheel-rail interaction | Wheel-rail | 355.9 | -7.43 |
| Rear wheel-rail interaction | wheel-rail | -355.9 | -7.43 |
| ● Car 2 | | | |
| Drawbar connection to car in front | Draft gear (Type 2) | 306.0 | -25.03 |
| Drawbar connection to car in rear | Draft gear (Type 1) | -306.0 | -25.03 |
| Front end sill/anticlimber | Anticlimber | 355.9 | 5.97 |
| Rear end sill/anticlimber | Anticlimber | -355.9 | 7.47 |
| Front wheel-rail interaction | Wheel-rail | 355.9 | -7.43 |
| Rear wheel-rail interaction | Wheel-rail | -355.9 | -7.43 |

The element connection data for the remaining pairs of cars in the loaded consist is identical to that given above for the first pair.

27

TABLE 6.-PHYSICAL PROPERTIES OF ELEMENTS

**Draft Gear (Type 1)**

| | | | |
|---|---|---|---|
| Initial stiffness | = 12,000 lb/inch | Hysteresis load | = 10,000 lb |
| Travel | = 2.50 inch | Pin shear load | = 150,000 lb |
| Stiffness after bottoming | = 160,000 lb/inch | Postshear travel | = 2.75 inch |
| | | Fracture load | = 250,000 lb |

**Draft Gear (Type 2)**

| | | | |
|---|---|---|---|
| Initial stiffness | = 12,000 lb/inch | Hysteresis load | = 10,000 lb |
| Travel | = 2.50 inch | Pin shear load | = 150,000 lb |
| Stiffness after bottoming | = 160,00 lb/inch | Postshear load | = 30.0 inches |
| | | Fracture load | = 250,000 lb |

**Anticlimber**

| | | | |
|---|---|---|---|
| Vertical elastic stiffness, end K | = 175,000 lb/inch | Vertical elastic stiffness, end $\ell$ | = 175,000 lb/inch |
| Vertical plastic stiffness, end K | = 1633 lb/inch | Vertical plastic stiffness, end $\ell$ | = 1,633 lb/inch |
| Vertical yield deflection, end K | = 0.20 inch | Vertical yield deflection, end $\ell$ | = 0.20 inch |
| Vertical rupture deflection, end K | = 5 inches | Vertical rupture deflection, end $\ell$ | = 5 inches |
| Horizontal elastic stiffness, end K | = 4,450,000 lb/inch | Horizontal elastic stiffness, end $\ell$ | = 4,450,000 lb/inch |
| Horizontal plastic stiffness, end K | = 20,620 lb/inch | Horizontal plastic stiffness, end $\ell$ | = 20,620 lb/inch |
| Horizontal yield deflection, end K | = 0.053 inch | Horizontal yield deflection, end $\ell$ | = 0.053 inch |
| Horizontal rupture deflection, end K | = 56 inches | Horizontal rupture deflection, end $\ell$ | = 56 inches |
| Torsional elastic stiffness, end K | = 110,800 inch-lb/rad | Torsional elastic stiffness, end $\ell$ | = 110,800 inch-lb/rad |
| Torsional plastic stiffness, end K | = 25,500 inch-lb/rad | Torsional plastic stiffness, end $\ell$ | = 25,500 inch-lb/rad |
| Torsional yield deflection, end K | = 0.001 rad | Torsional yield deflection, end $\ell$ | = 0.001 rad |
| Torsional rupture deflection, end K | = 1 rad | Torsional rupture deflection, end $\ell$ | = 1 rad |
| Face height, end K | = 6 inches | Face height, end $\ell$ | = 6 inches |
| Length, end K | = 58.125 inches | Length, end $\ell$ | = 58.125 inches |

**Wheel-Rail**

| | | | |
|---|---|---|---|
| Spring constant deflection < $\delta_L$ | = 4,100 lb/inch | Wheel radius | = 23.362 inches |
| Spring constant deflection > $\delta_L$ | = 6,468,000 lb/inch | Damping constant | = 1,000 lb-sec/inch |
| $\delta_L$ | = 12.362 inches | | |

## 3. CONSIST MODEL COMPUTER RESULTS

The initial model described in Section 2 was input to the IITRAIN computer code to simulate the primary collision of two impacting consists of urban railcars. The unloaded eight-car consist was given an initial velocity of 20 mph just prior to impact with the loaded motionless eight-car consist. Figure 5 shows the horizontal accelerations for all of the cars of both the impacting and impacted cars. The vertical and rotation accelerations of the leading cars of the two consists are shown in Figures 6,7,8 and 9. All accelerations were taken at the c.g. of the car bodies.

The simplified model described in Section 2 was also input to the IITRAIN computer code to simulate a 20 mph collision identical to the simulation using the initial model. Figure 10 shows a comparison of the horizontal accelerations for the simplified model and the initial model for the first 200 msec of the collision. The simplified model was then used to simulate a 35 mph collision of an unloaded consist into a standing loaded consist. Figure 11 shows the horizontal accelerations of all of the cars of both the impacted and impacting trains.

Finally, a simulation of the collision of only the leading cars of the initial model was conducted. The unloaded leading car collided with the loaded car at 20 mph. A comparison of the horizontal accelerations for this simulation with the accelerations for the initial model consist collision is given in Figure 12.

### Discussion of Results

The horizontal acceleration results given in Figure 5 for the detailed model of a 20 mph collision show that all the cars are subject to an essentially rectangular acceleration pulse. The average accelerations are 5 g and 3 g, respectively, for the leading impacting cars of the moving unloaded consist and the stationary loaded consist. The remaining cars are subject to average accelerations of 4 g and 2.5 g, respectively, for the unloaded and loaded consists.
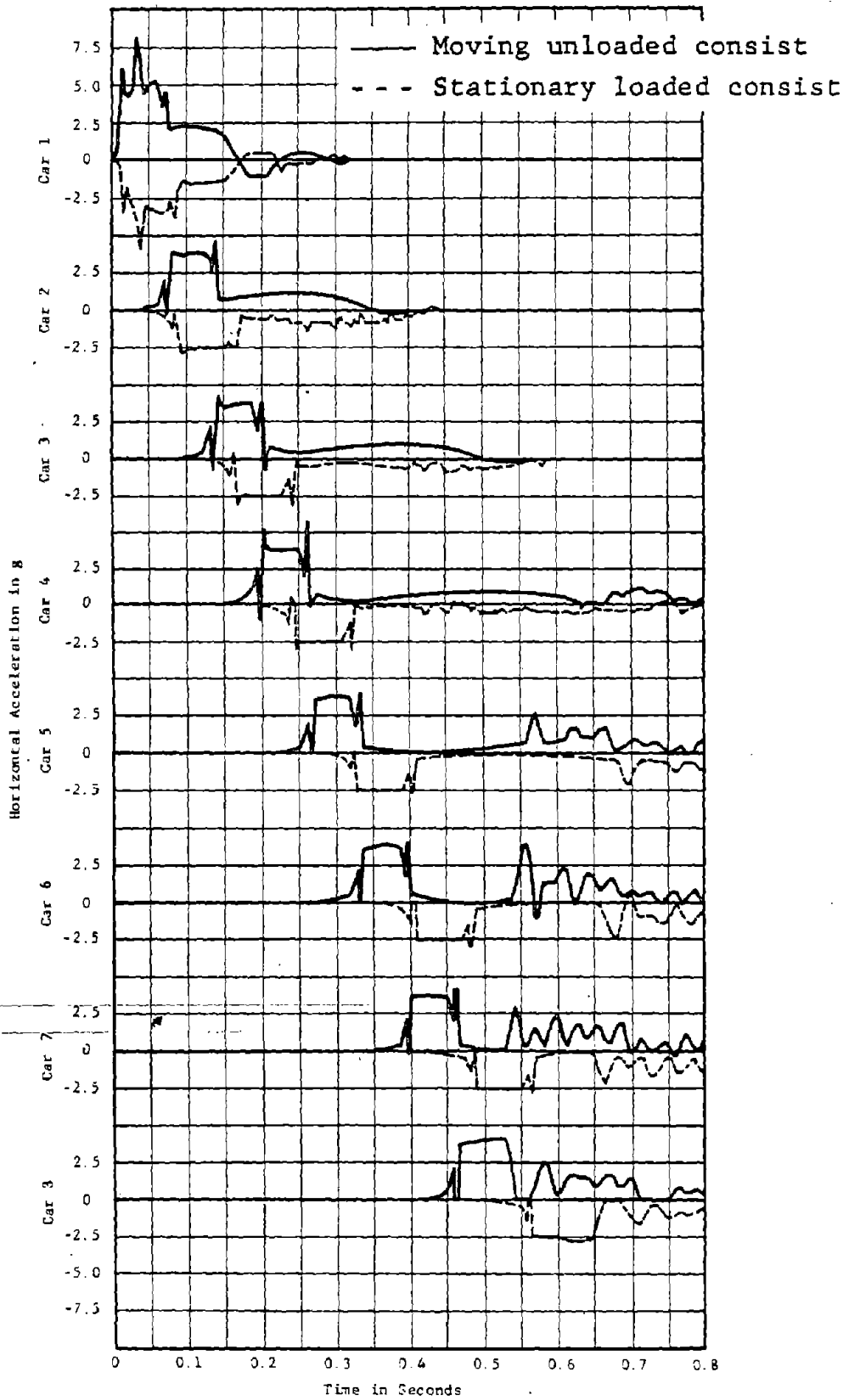
29

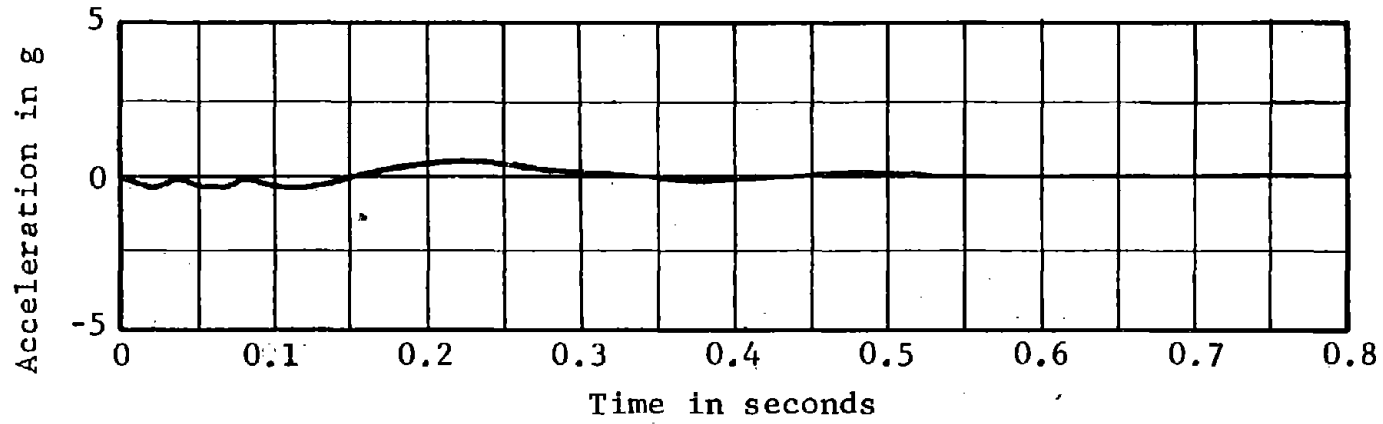FIGURE 5. INITIAL MODEL HORIZONTAL ACCELERATIONS

30

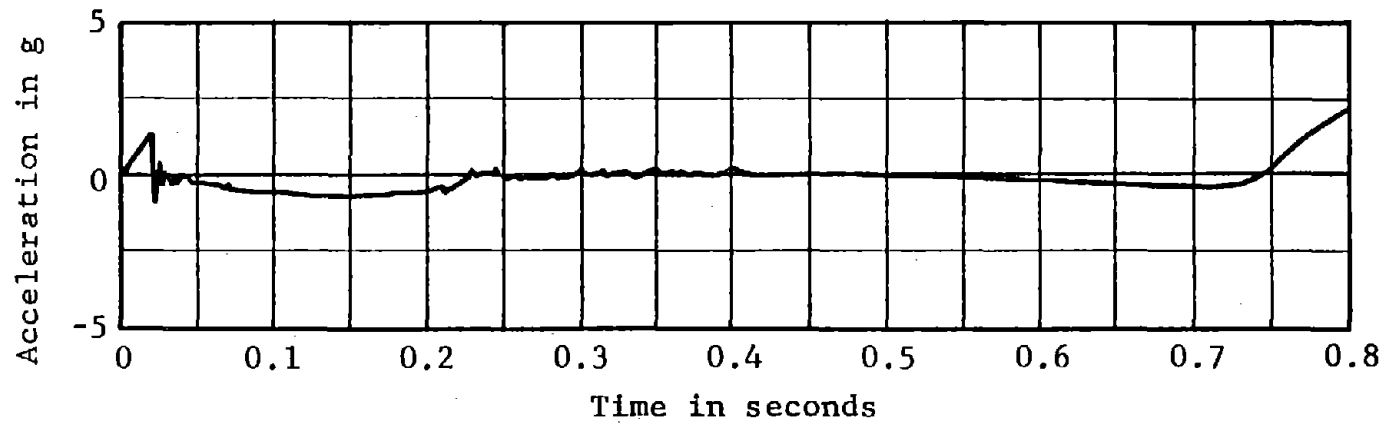FIGURE 6. INITIAL MODEL VERTICAL ACCELERATION OF IMPACTING CAR (Moving consist)



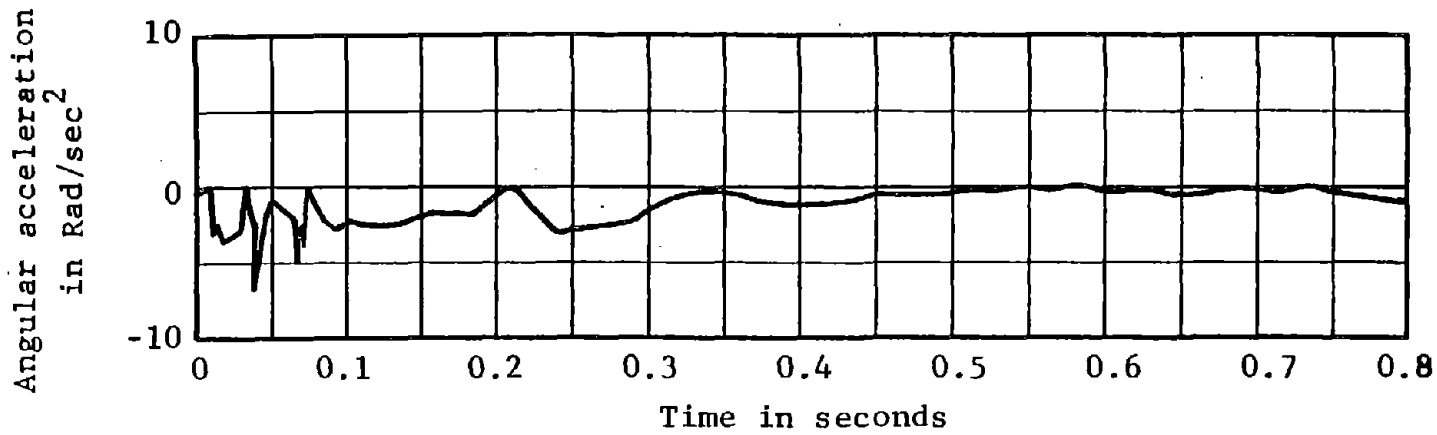FIGURE 7. INITIAL MODEL VERTICAL ACCELERATION OF IMPACTED CAR (Stationary consist)

31

FIGURE 8. INITIAL MODEL ANGULAR ACCELERATION OF IMPACTING CAR
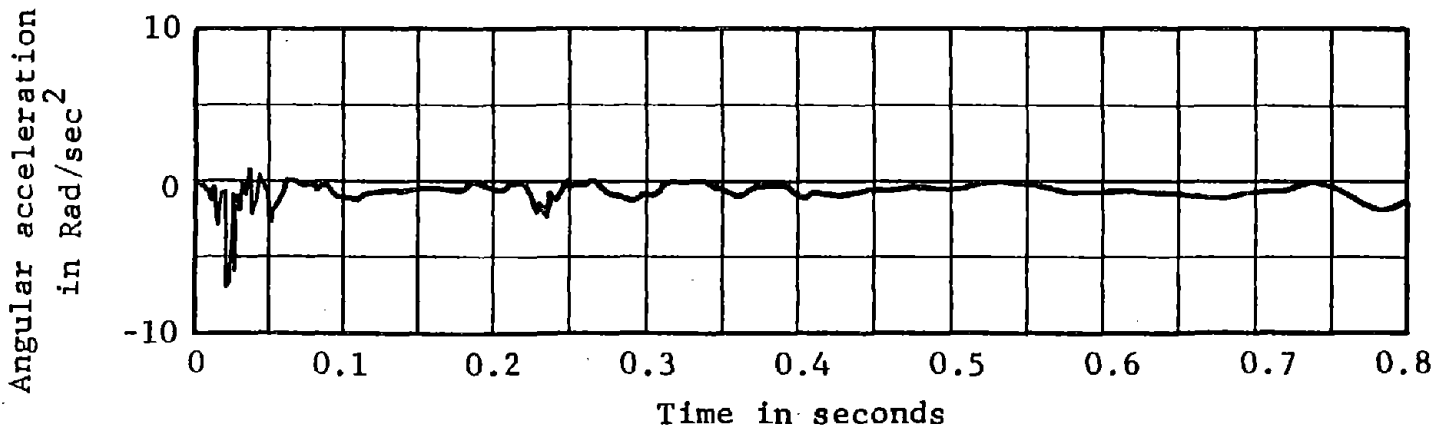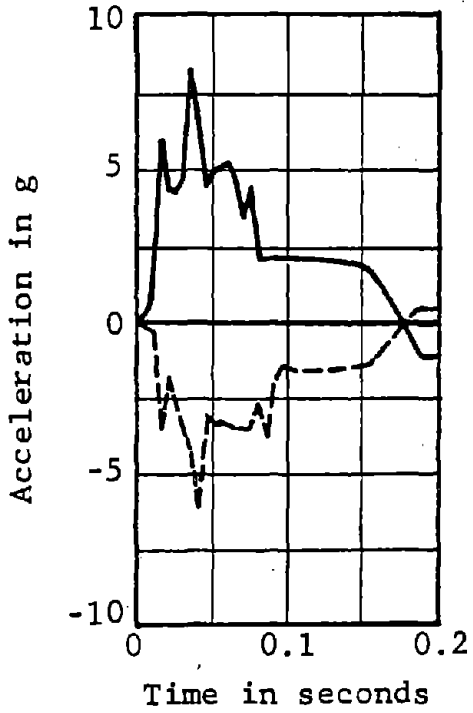(Moving consist)

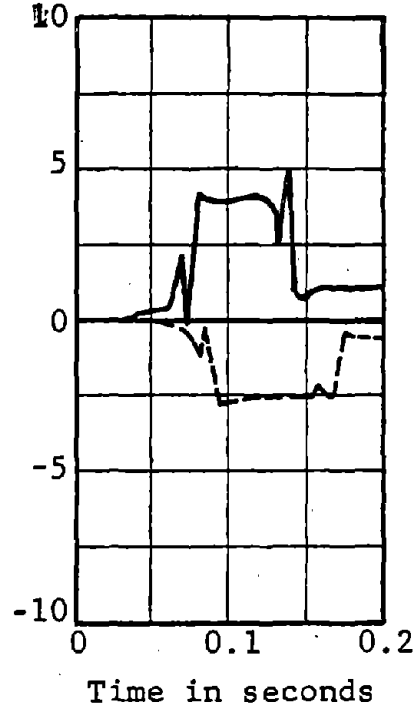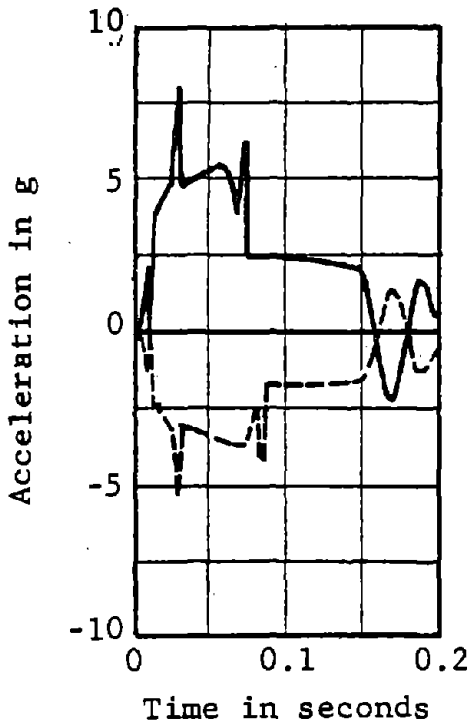FIGURE 9. INITIAL MODEL ANGULAR ACCELERATION OF IMPACTED CAR
(Stationary consist)

FIGURE 10.   COMPARISON OF HORIZONTAL ACCELERATIONS
FOR INITIAL AND SIMPLIFIED CONSIST MODELS

FIGURE 11. SIMPLIFIED MODEL HORIZONTAL ACCELERATIONS

34

—— Moving unloaded consist
- - - Stationary loaded consist
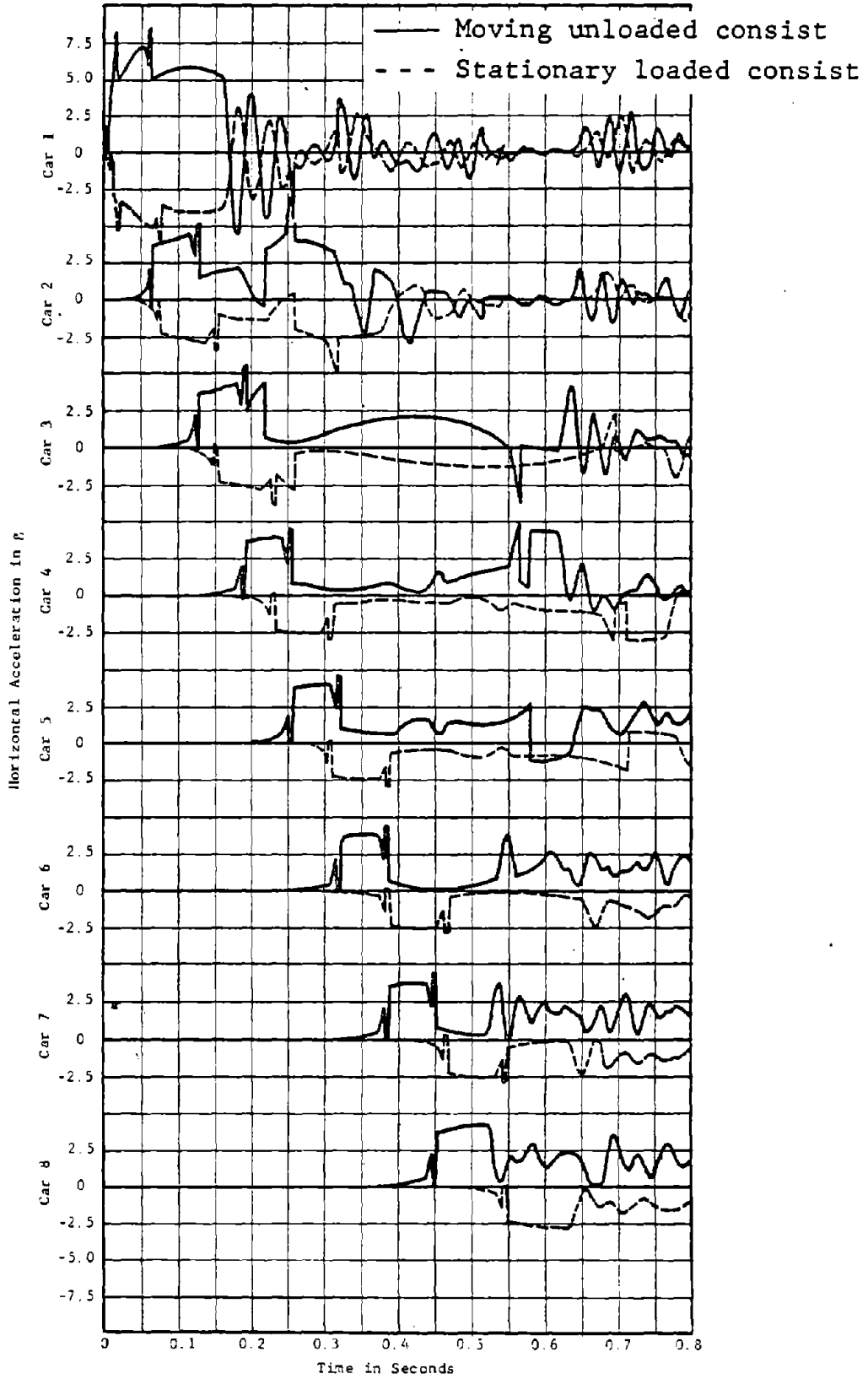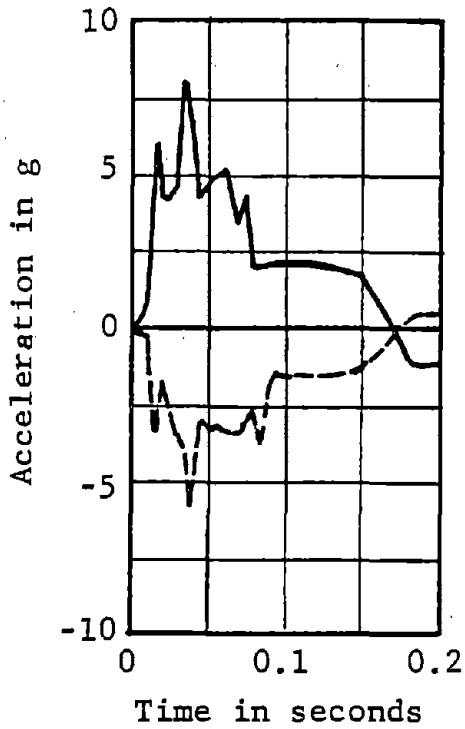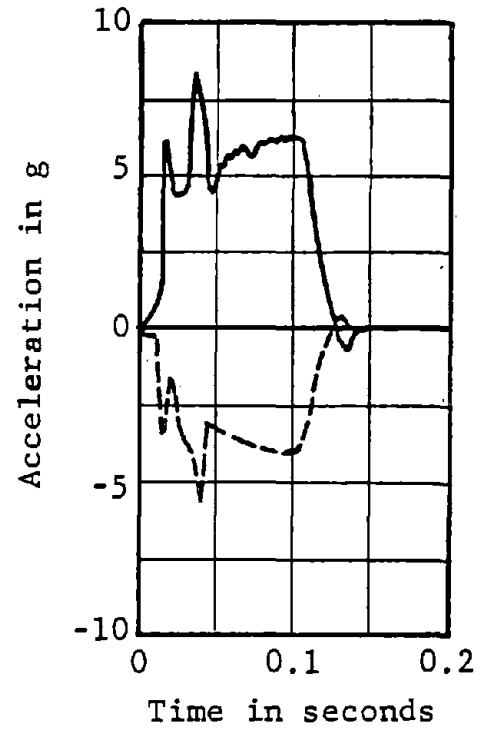


Car 1  Initial Model                    Single Car Collision

FIGURE 12   COMPARISON OF HORIZONTAL ACCELERATIONS
FOR INITIAL CONSIST MODEL AND SINGLE CAR COLLISION

The pulse duration is approximately 67 msec for the unloaded consist and 80 msec for the loaded consist. As might be surmised, the 4 g and 2.5 g accelerations correspond to the ratio of the horizontal yield force for the anticlimbers to the weights of the unloaded and loaded transit cars. Also the 67 and 80 msec time durations correspond to the time required for the anticlimbers of adjacent cars to engage at these acceleration levels.

The vertical and angular (pitch) accelerations for the 20 mph collision are found to be relatively low as shown in Figures 6 through 9. These low accelerations indicate that vertical and pitch motions have little direct effect on passenger injury in a 20 mph collision. However, when these motions are combined with the horizontal acceleration, their effect may be appreciable.

Only minor differences exist between the accelerations computed for the simplified consist model and the initial consist model as shown in Figure 10. This is especially true of the cars after the two leading impacting cars. The impacting cars have slightly different peaks but the average accelerations are identical. It can be concluded from these results that the simplified model is adequate for use in studying transit car collisions. Since the simplified model requires appreciably less computer time, large savings can be realized from its use.

The horizontal acceleration results given in Figure 11 for the simplified model of a 35 mph collision again show the cars are subject to essentially rectangular acceleration pulses. The average accelerations are the same as for the 20 mph collision, 5 g and 3 g respectively, for the leading impacting cars of the unloaded and loaded consists and 4 g and 2.5 g, respectively for the remaining cars of these two consists. The leading impacting cars have a much larger pulse duration (approximately 150 msec each) than for the 20 mph collision. However, the remaining cars have the identical pulse durations, 67 and 80 msec, respectively, for the unloaded and loaded cars.

36

There is a tendency for a second rectangular pulse for some of the cars in the 35 mph collision, in particular, cars 2 and 4 of both consists. There are also other short duration acceleration pulses not evident in the lower speed collision.

The comparison of the horizontal accelerations for the initial eight-car consist model collision at 20 mph and the collision of two single cars (also at 20 mph) shown in Figure 12, shows approximately the same peak and average accelerations. Only the time durations of the pulses are different. This is due to the anti-climbers of the cars in the consist engaging, thus reducing the accelerations of the impacting cars.

# 4. GENERATION OF FORCE-DEFORMATION RELATIONSHIPS

## 4.1 Finite Element Procedure

The response of urban railcar structures under crash loadings is a complex process primarily involving:

- transient, dynamic behavior
- complicated framework and shell assemblages
- large deflections and rotations
- extensive plastic deformation.

Previous attempts at a formal analysis of this process have been only partly successful due to a variety of limitations which, in particular instances, have included inadequacies in element formulations, material representations or solution procedures. The technique presented in this report represents an attempt to develop a finite element program which is specifically tailored to the class of problems inherent in vehicle crash response, and which employs or extends current avenues in finite element analysis which seem best suited to such problems. The field of nonlinear finite element analysis is currently an extremely active area of research with an extensive, related literature and a variety of methods and approaches. Consequently, a formal review of the field as background for the analysis approach presented here is not attempted. Instead, major features of this technique are briefly described, and some rationale is offered for their use in the context of urban railcar analysis.

The principal feature of the finite element analysis employed in this work (see Ref. 1) is found in the treatment of large deflections. A coordinate system is defined for each finite element which rotates and translates with the element and serves as a reference system in which element shape functions and local displacements and forces are established.

As indicated in Figure 13, three coordinate systems are used
to define the deformed position of the element:

1. A global system (X, Y, Z) is used to define the
   deformed and undeformed positions of nodes and serves
   as an inertial reference system for translational
   motions.

2. A nodal system $(\overline{X}, \overline{Y}, \overline{Z})$ coincides with the principle
   axes of the lumped masses at each node point and
   rotates with the mass point during deformation. The
   components of any vector, $\overline{v}$, transform from nodal to
   global systems by the time varying transformations

   $$\{V\} = [\lambda]\{\overline{v}\}$$

   where the elements of $\lambda$ are obtained from the
   equations of rotational motion at each time step.

3. An element system $(\hat{X}, \hat{Y}, \hat{Z})$ is embedded in each
   element, and serves as a reference for element
   distortion and forces. A vector, $\hat{v}$, transforms from
   the element to global system by the time varying
   transformation

   $$\{V\} = [\mu]\{\hat{v}\}$$

   where the elements of $\mu$ are determined by the
   displaced position of the element at each time step.

The solution procedure is based on the calculation of forces
and moments acting on the element nodes arising due to correspond-
ing nodal displacements and rotations. All such quantities, as
well as element displacement functions, are defined with respect to
the element coordinate system. Thus, for sufficiently small
elements, the rotations in the element systems may be assumed to be
sufficiently small to admit displacement functions appropriate to a
small displacement element formulation.

The first step in the process involves the calculation of
displacements and rotations in the element system. Having obtained
these quantities, corresponding forces and moments are found from
appropriate volume integrations of the resulting stress fields.
This process makes use of the assumed displacement fields
corresponding to a small or moderate rotation element formulation
to obtain strains within the element and an elasto-plastic stress
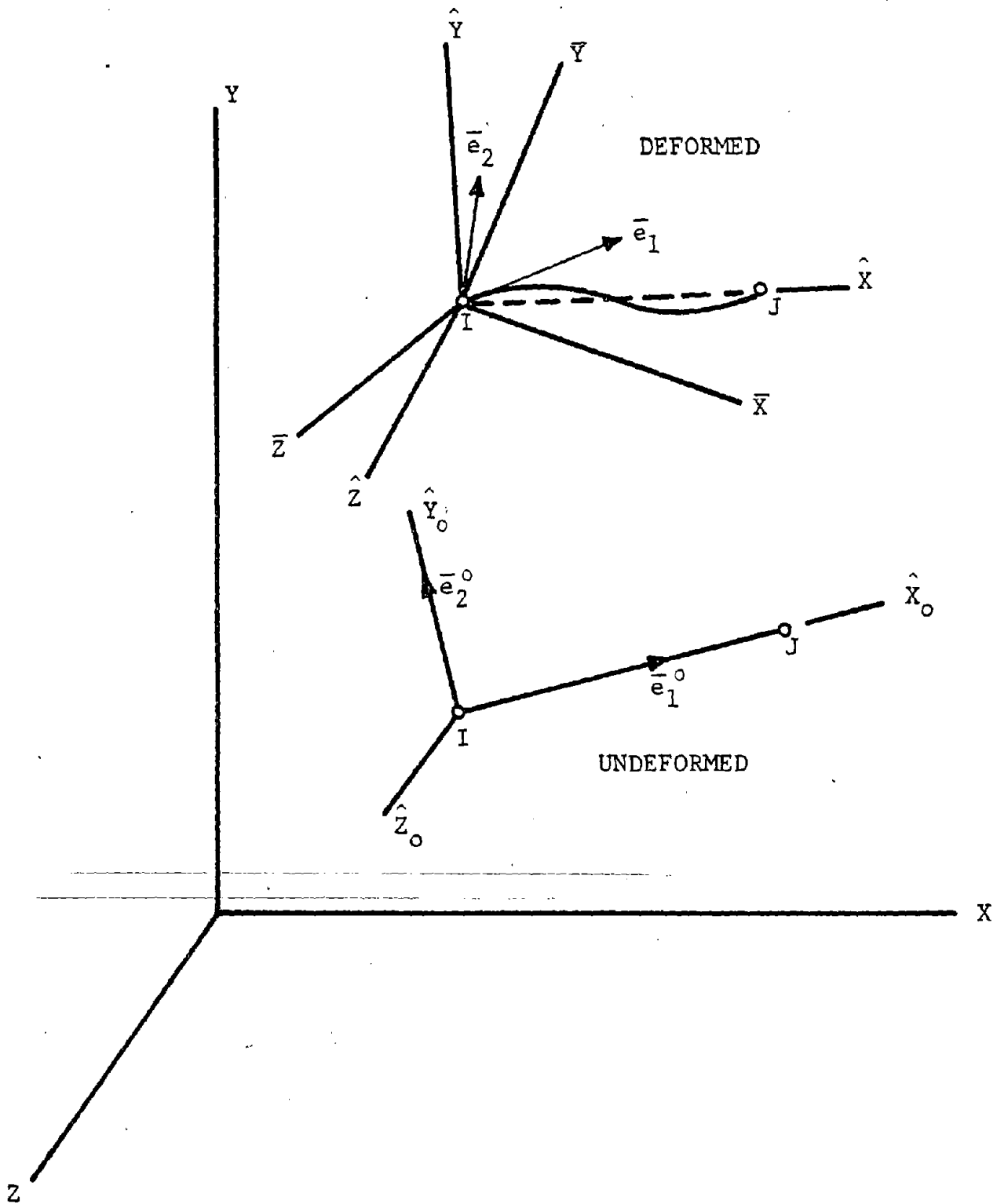law relation. The forces, $\hat{f}$, and moments, $\hat{m}$, acting on the element

FIGURE 13.   THREE-DIMENSIONAL BEAM FINITE ELEMENT
AND COORDINATE SYSTEMS

40

nodes are subsequently transformed to the global and nodal system, respectively, by means of the transformations

$$\{f\} = [\mu] \{\hat{f}\}$$

$$\bar{m} = [\lambda]^T [\mu]\{\hat{m}\}$$

The equations of motion (obtained from Newton laws) at a node point for both translations and rotations are written as

$$[M][a_{i+1}] = [F^E_{i+1}] - [F^I_i] - [K][\Delta x] \tag{1}$$

where

[M] – diagonal lumped mass matrix for the node

[a] – acceleration vector for the node referred to the global axes

$[F^E]$ – vector of external loads at the node referred to the global axes

$[F^I]$ – vector of internal forces at the node referred to the global axes

[K] – tangent stiffness matrix for the element

[$\Delta x$] – increment in displacement and rotation for the element from step i to step i+1.

The numerical technique employed to integrate the equations of motion consists of the Newmark-beta method (Ref. 2). This method relates displacement, $\Delta x$, velocity, v, and acceleration, a, at the beginning, i, and end, i+1, of a time interval, h, by the relations

$$\Delta x = v_i h + (1/2 - \beta) a_i h^2 + \beta h^2 a_{i+1} \tag{2}$$

$$v_{i+1} = v_i + h/2 (a_i + a_{i+1}) \tag{3}$$

where $\beta$ is an assumed parameter related to the behavior of the acceleration during the time interval.

The solution procedure in the computer program combines the Newmark-beta recurrence formulas and the equations of motion in the following manner: substituting equation (1) and (2) and rearranging yields

$$[K + \frac{M}{\beta h^2}] \Delta x = F^E_{i+1} - F^I_i + M \left[ \frac{v_i}{\beta h} + \frac{(1-2\beta)}{2\beta} a_i \right]$$

or simply

$$[K^{eff}][\Delta x] = [F^{eff}] \tag{4}$$

Equation (4) is solved at every time step for $[\Delta x]$. Velocities and accelerations are subsequently obtained from equations (3) and (2) respectively.

One noteworthy aspect of the procedure is the stability and accuracy of the procedure for large values of the time step. Although other procedures are available that require fewer computations per time step, they are restricted to time steps on the order of the axial transit time for the smallest element in the system. The previously developed procedure admits much larger time steps without deterring from the accuracy of the computations. However, indiscriminately large time steps will cause the solution to diverge.

When the external load experienced by any given member is applied gradually, whether it be an applied force or displacement field (both of which are admissible with this formulation), the computer program can simulate a quasi-static crush test. This procedure can be employed to generate force-deformation relationships for major subassemblages. As a demonstration of the accuracy and applicability of this finite element technique, the following example problem is presented.

Figure 14 illustrates a shallow arch problem which exhibits a nonlinear equilibrium path which leads to snap-through buckling. Results from the current effort are compared to those obtained by Mallet and Haftka (Ref. 3). A vertical displacement of 0.25 inch in increments of 0.025 inch was applied to the crown of the arch. The resultant force at the crown as a function of the imposed displacement is shown in Figure 15. The work used as a comparison basis was also based upon a nonlinear finite element analysis using asymptotic solution techniques. As can be readily seen, the results are in good agreement. Of particular significance in this problem is the unloading and reloading action between 0.10 and 0.20 inch.

R = 10. in.
θ = 20 deg
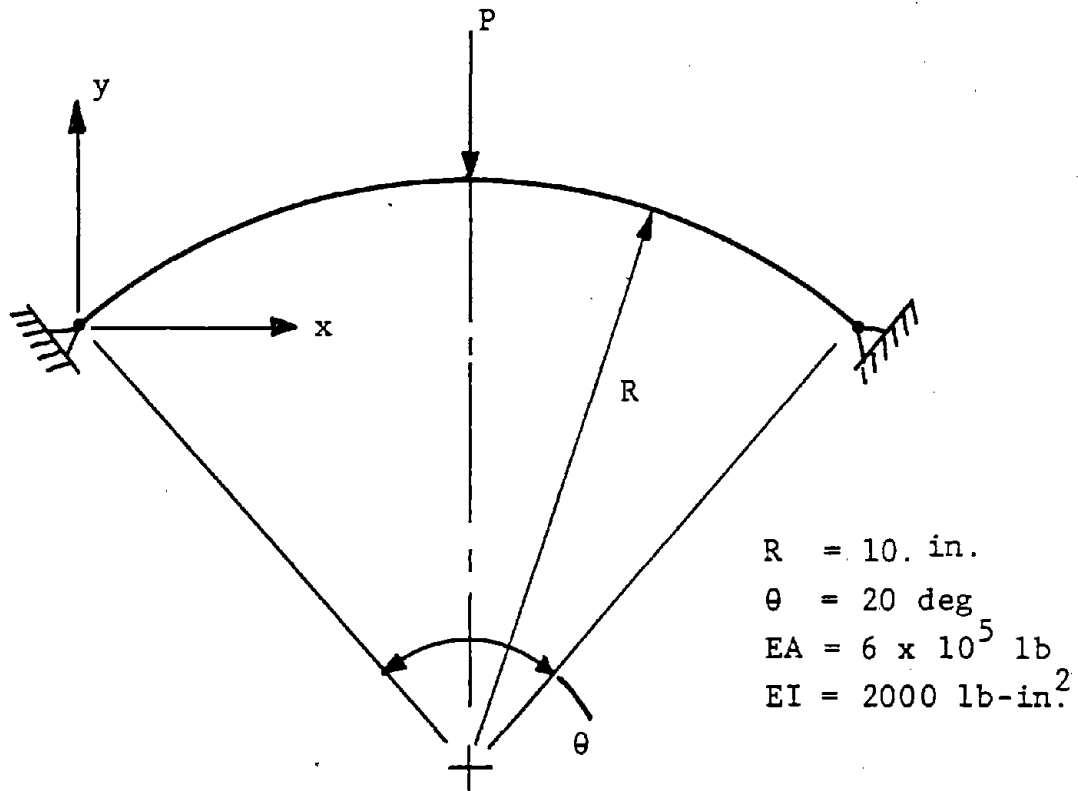EA = $6 \times 10^5$ lb
EI = 2000 lb-in²

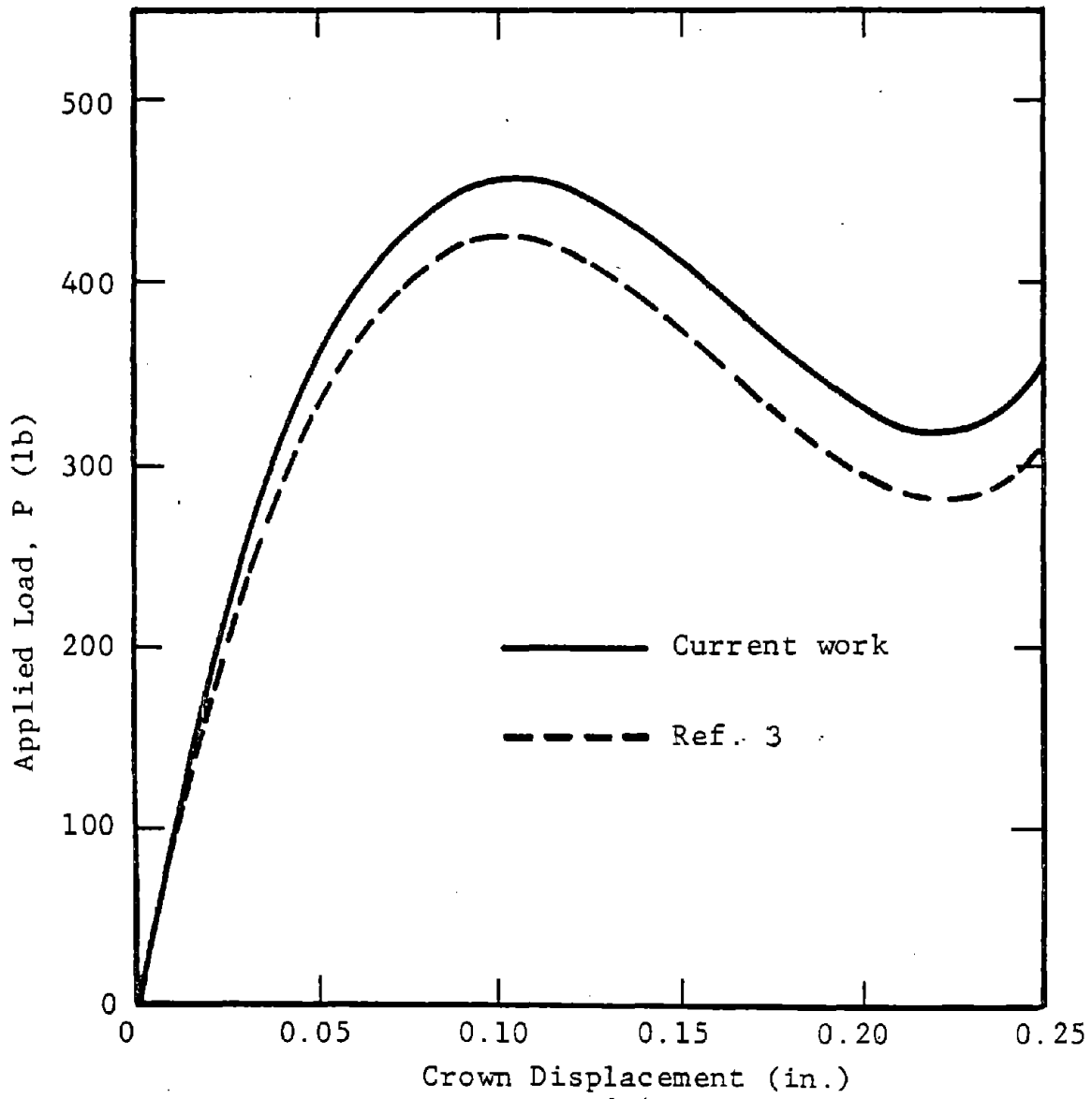FIGURE 14.   POINT LOADED HINGED CIRCULAR ARCH (REF. 3)

FIGURE 15.  FORCE-DEFLECTION CURVE FOR HINGED CIRCULAR ARCH

The use of a finite element procedure is best illustrated with an actual application of a finite element computer program to obtain force-deformation relationships for a typical transit car subassemblage. The use of the WRECKER II[*] computer code to obtain such force-deformation relationships is described in Sections 4.1.1 and 4.1.2. Two alternate procedures are illustrated in these sections. In Section 4.1.1, forces are input to a typical end sill structure and the resulting deflections are computed. The deflections are input to a typical end of car superstructure and the required forces are calculated in Section 4.1.2.

4.1.1 <u>Application to End Sill Structure</u> - Figure 16 is a schematic of the end sill subassembly for a typical transit car. This subassembly includes the end sill, the side sills, the draft sill and the anticlimber. The engineering drawings for a transit car end sill structure presently in operation were obtained and a finite element model of this structure was devised for the WRECKER II (Ref. 1) computer code. A schematic of this model showing the 26 nodes and 24 beam elements required for an accurate representation of the structure is shown in Figure 17. Since the structure and loadings are symmetrical about the centerline of the car only half of the end sill was modeled and appropriate boundary conditions were imposed on the centerline nodes (nodes 17 through 26).

All the beams in this model were simulated with elastic-plastic beam elements. The material properties for all these beams were taken to be the properties of A36 steel. Five different cross-sectional geometries were necessary to describe the various beams. Beams 1 through 6 had the cross-sectional properties of the transit car side sills. The anticlimber and end sill structure provided the properties for beams 7 through 10.

---

[*]The WRECKER II computer code was developed at IIT Research Institute for the Department of Transportation, National Highway Traffic Safety Administration under Contract DOT-HS-6-01364 and is described in Reference 1.
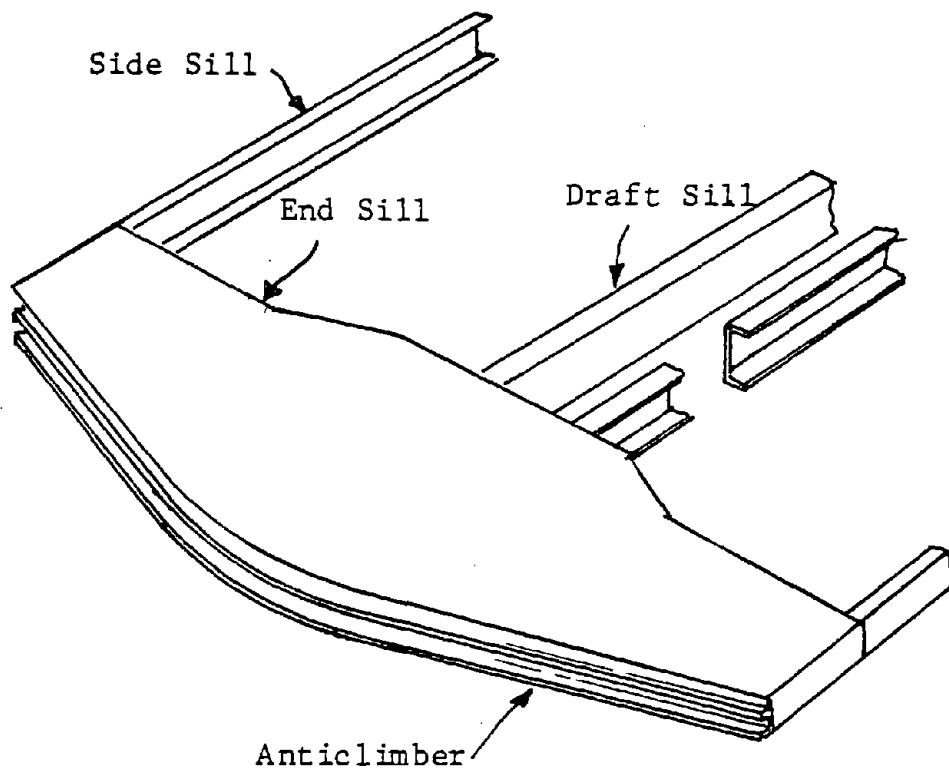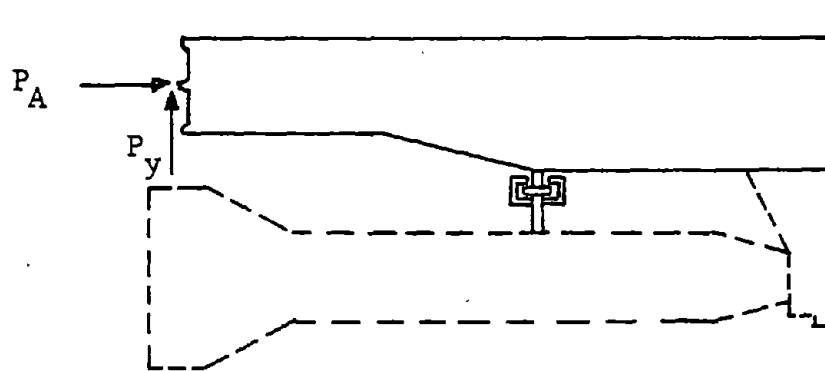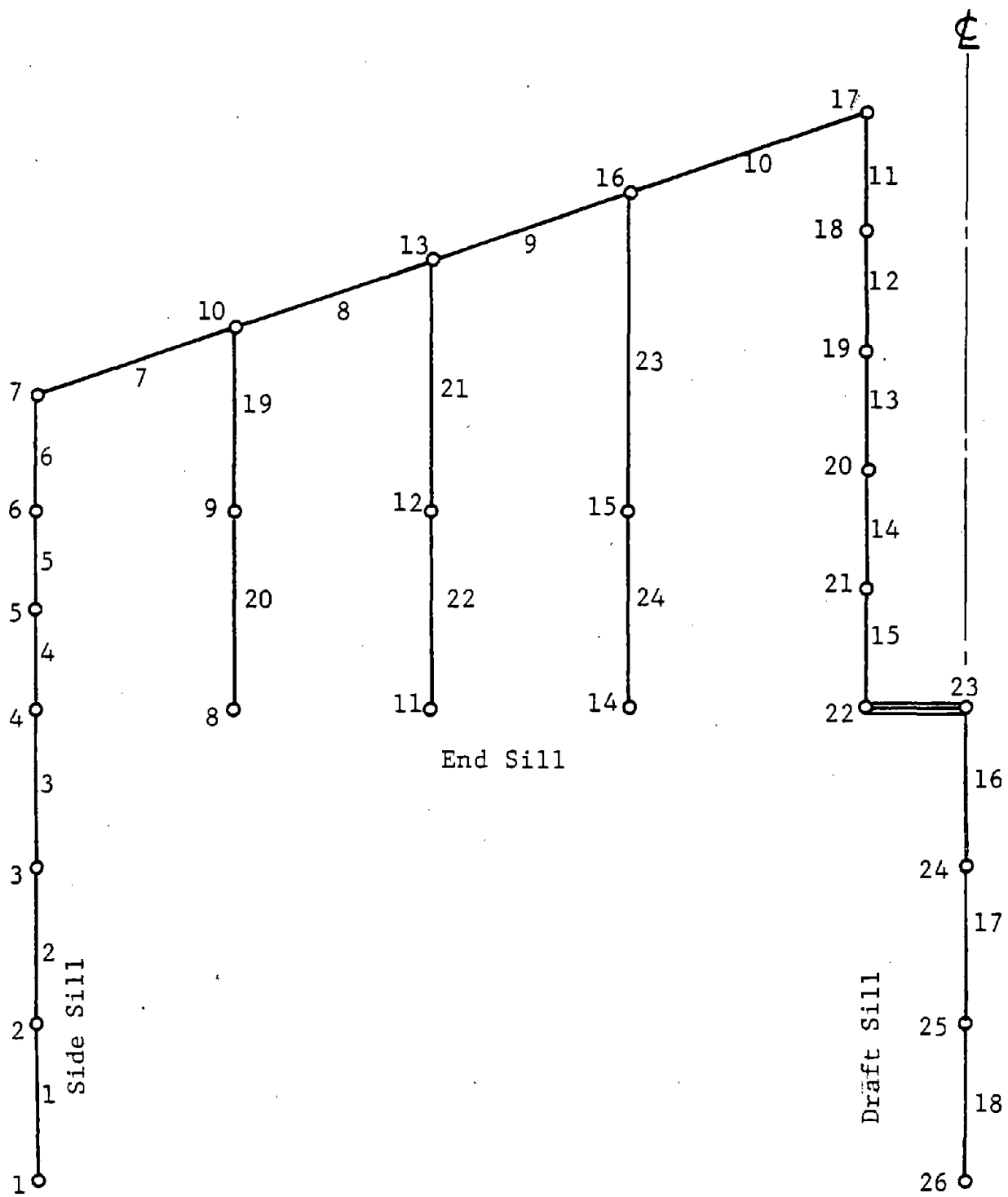
45

FIGURE 16. END SILL STRUCTURAL SUBASSEMBLY

46

FIGURE 17. FINITE ELEMENT MODEL OF END SILL

Beams 11 through 15 modeled beam structure in the end sill while beams 16, 17 and 18 had the cross-sectional properties of the draft sill. The top and bottom plate structure of the end sills were simulated with beams 19 through 24.

In this model nodes 1, 8, 11, 14 and 26 were completely restrained representing the boundary of the structural subassemblage being investigated. Force was slowly applied at node 17 in steps of 500 lb/sec for the vertical load crush characteristics and 4000 lb/sec for the buff load crush characteristics. The resulting vertical and horizontal deflections, respectively, of node 17 were calculated. The resulting force-deformation characteristics for the end sill subassemblage are given in Figures 18 and 19. Calculations were carried out until the computer analysis "blew up" indicating the structure had reached its maximum load carrying capacity. Since forces were being input as an increasing function the decrease in the load carrying capacity after maximum load is attained could not be calculated.

4.1.2 <u>Application to End of Car Superstructure</u> - Figure 20 is a schematic of the end of car superstructure for a typical transit car. This subassembly includes the collision posts, side sills, cove sills, purlins and carlines located in the space between the end of the car and the body bolster. The engineering drawings for a transit car end of car superstructure presently in operation were obtained and a finite element model of this structure was devised for the WRECKER II (Ref. 1) computer code. A schematic of this model showing the 35 nodes and 50 beam elements required for an accurate representation of the structure is shown in Figure 21. Since the structure and loading is symmetrical about the centerline of the car only half of the end of car superstructure was modeled and appropriate boundary conditions were imposed on the centerline nodes (nodes 7, 14, 21, 28, 29 and 34).

All the beams in this model were simulated with elastic-plastic beam elements. The material properties of the side sills were for A36 steel while the remaining structure was aluminum.
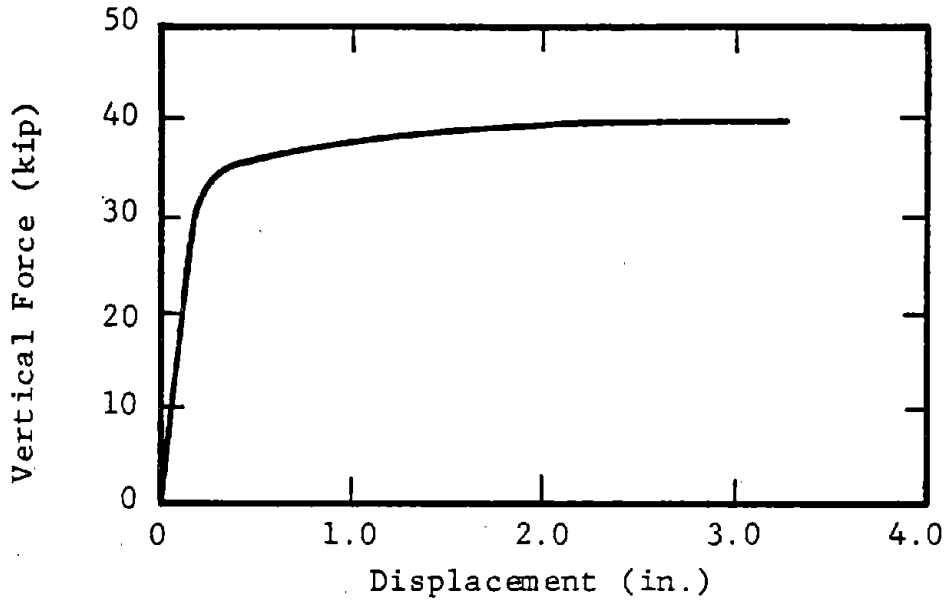
48

FIGURE 18.   END SILL VERTICAL LOAD CRUSH CHARACTERISTIC



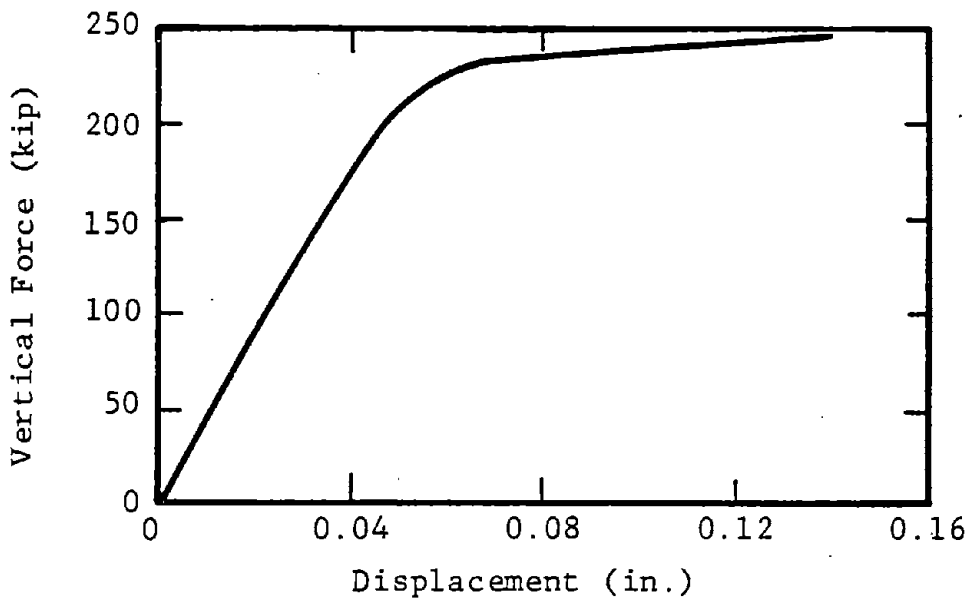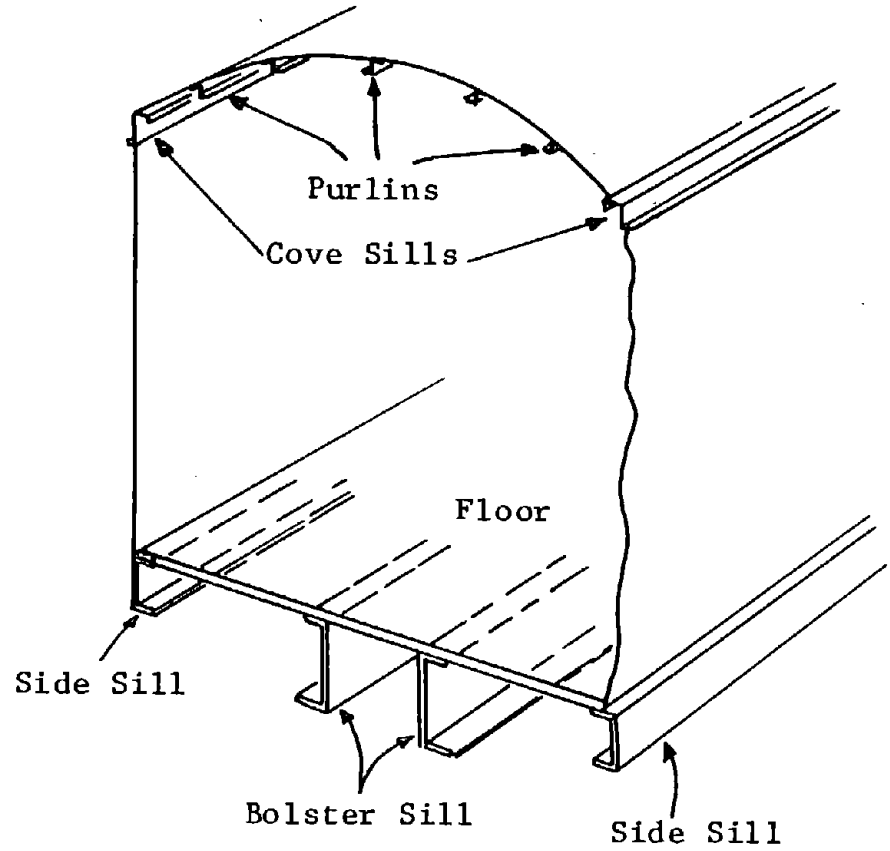FIGURE 19.   END SILL BUFF LOAD CRUSH CHARACTERISTIC

Collision Post

P

End Sill

Purlins

Cove Sills
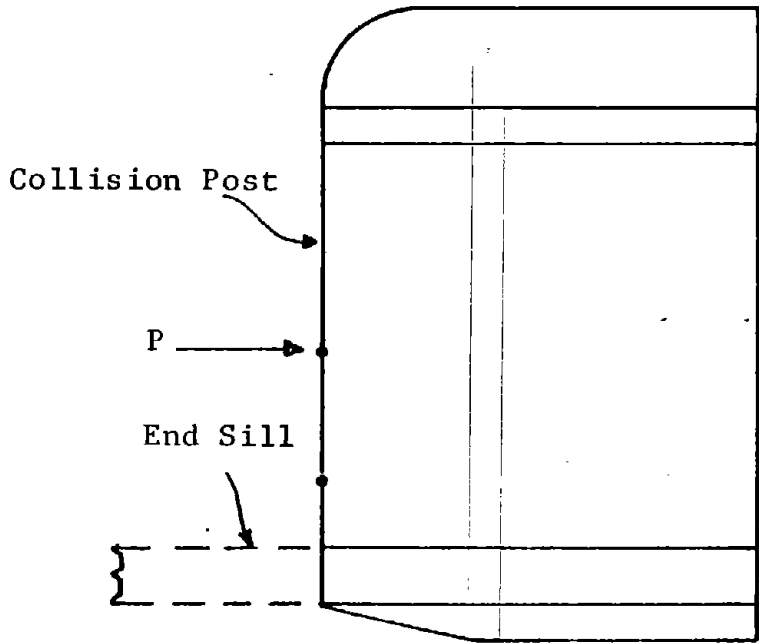
Floor

Side Sill

Bolster Sill

Side Sill

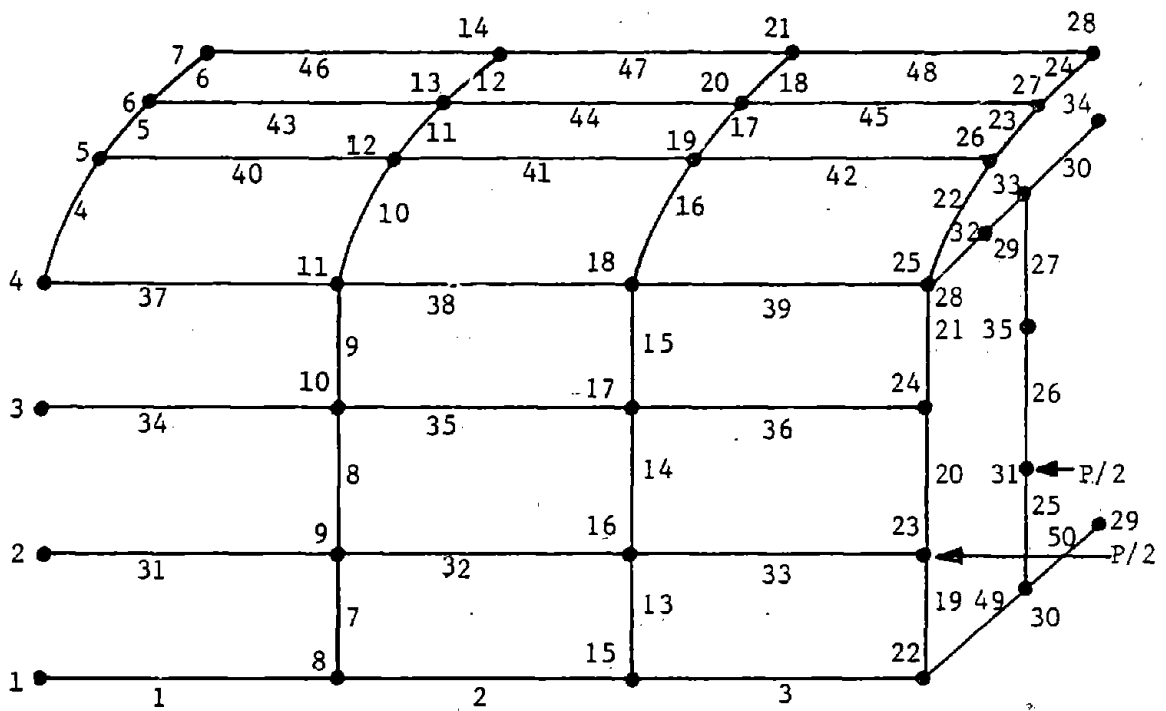FIGURE 20.   END OF CAR SUPERSTRUCTURE

50

FIGURE 21. FINITE ELEMENT MODEL OF END OF CAR SUPERSTRUCTURE

51

Nine different cross-sectional geometries were required to describe the various beams. Beams 1, 2 and 3 had the cross-sectional properties of the side sills. The carline properties were used for beams 4, 5, 6, 10, 11, 12, 16, 17, 18, 22, 23 and 24. Beams 7, 8, 9, 13, 14 and 15 had properties corresponding to the vertical support members in the sides of the car body. The vertical support at the end of the car body provided the properties for beams 19, 20 and 21. Beams 25, 26 and 27 modeled the collision posts while 28, 29 and 30 modeled the horizontal structure above the collision posts at the end of the car. The longitudinal structural members in the sides of the car body provided the cross-sectional properties for beams 31 through 39. The car roof purlins provided the properties for beams 40 through 48. Finally beams 49 and 50 modeled the horizontal structure attaching the collision posts to the side sills of the car.

Nodes 1 through 7 of this model were completely restrained representing the boundary of the structural subassemblage being investigated. Horizontal displacements of nodes 23 and 31 were specified as a slowly varying function of time and the required total horizontal force was calculated. The resulting force-deformation crush characteristics for the end of car superstructure subassemblage is given in Figure 22. Calculations were carried out until the computer code calculations became unstable. A more slowly varying input displacement might have allowed calculation for a greater total deflection. However, sufficient data were obtained to show the decrease in the load carrying capacity of the structure which could not be obtained with the alternate procedure where force rather than displacement was input to the model.

## 4.2 Testing Techniques

4.2.1 Full-Scale Tests-The outlined test plan forms part of the methodology for generating the dynamic force-deformation relationships for structural subassemblages of critical modules of railcars. Specifically the problem of full-scale testing procedures of structural assemblages comprising such modules is addressed.
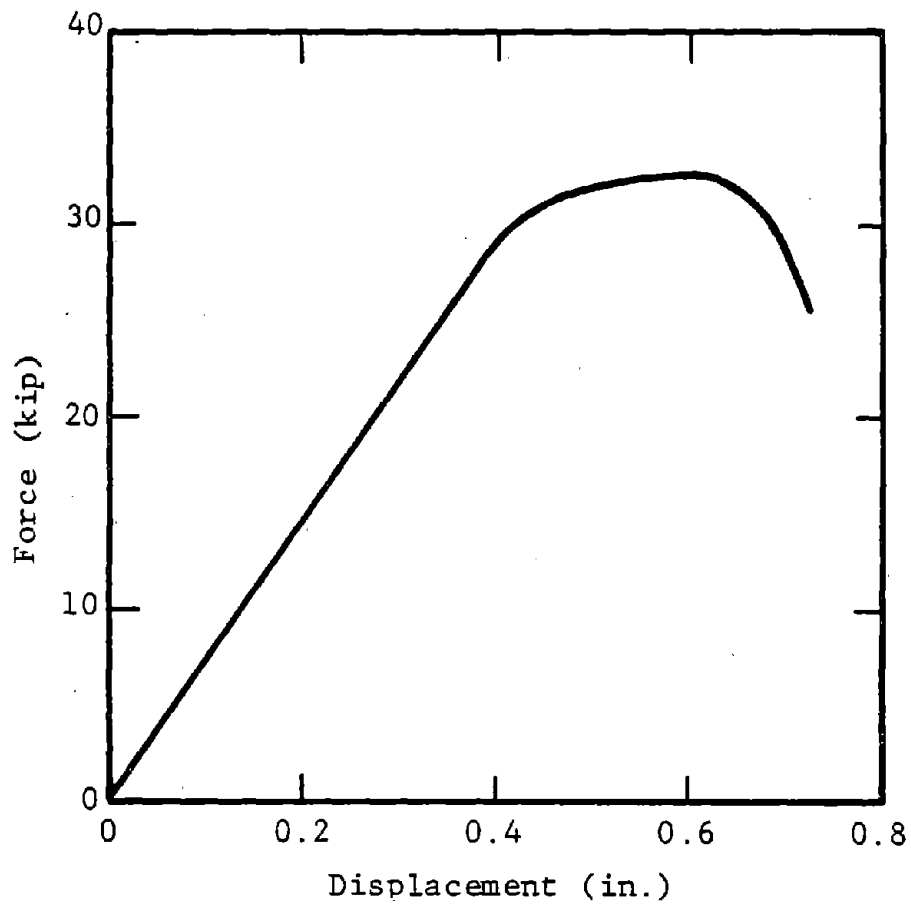
FIGURE 22.   END OF CAR SUPERSTRUCTURE CRUSH CHARACTERISTIC

The plan is to provide force-deformation test data characterizing the behavior of the assemblage under various load applications in its full extent of deformation, from load onset to full crush.

4.2.1.1 <u>Selection of Test Procedures</u>: The test procedure must yield useful application-oriented force-deformation test data. Conforming to this criterion, the test procedure selected will be one which yields data which can be used as input to analytic studies of railcar crashes. The IITRAIN computer program represents an advanced analytic tool for studying railcar crashes. Its input requirements can serve to indicate the type of test data useful to analytic studies of railcar crashes.

The IITRAIN program uses as input the nonlinear force-displacement curves characterizing the static behavior of critical railcar modules. With these, the program generates the dynamic force-deformation behavior as part of the solution of a specific railcar problem, using dynamic modeling of the modules involved. The static force-deformation behavior of a module in a railcar is basically unique, the dynamic one is not, since it varies with initial conditions, applied force-time history and the dynamics of interacting modules.

Figures 23 and 24 are examples of the static force-deformation curves for a railcar module used in analysis. Because of a lack of full-scale test data such curves are presently generated using finite element analysis or some other analytic method applied to the structure assembly, using individual member properties as input.

As indicated above, the use of static force-deformation curves is part of the methodology for generating the dynamic force-deformation relationships for structural subassemblages of critical modules of railcars. Therefore, the full-scale test procedures, formulated in subsequent sections, will be directed toward obtaining static force-deformation test data of specific critical subassemblage modules of railcars.
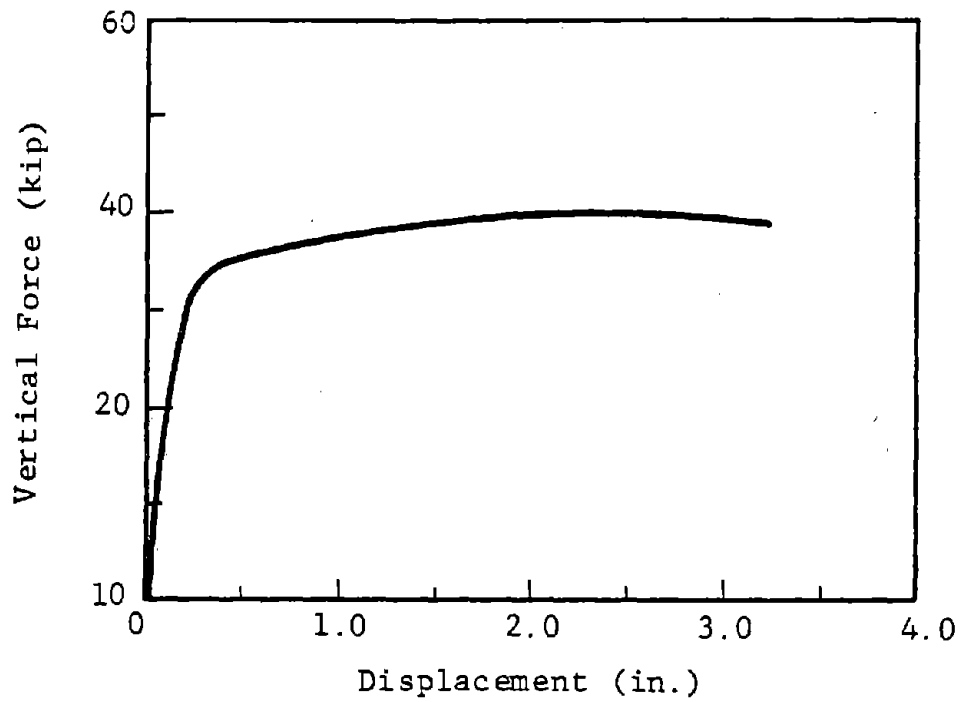
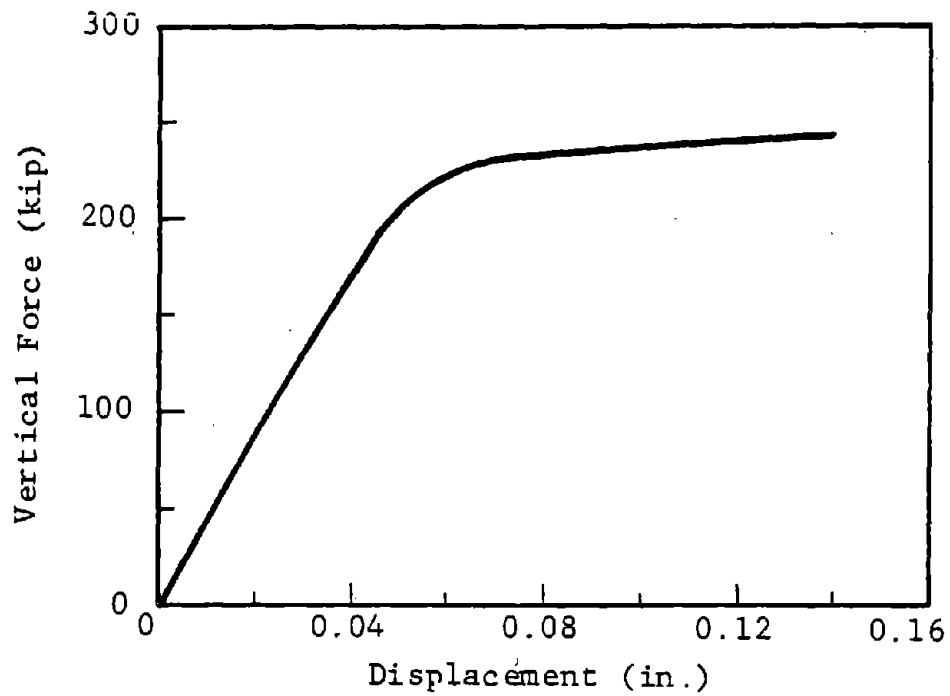FIGURE 23.   TYPICAL END SILL VERTICAL LOAD CRUSH CHARACTERISTIC



FIGURE 24.   TYPICAL END SILL BUFF LOAD CRUSH CHARACTERISTIC

The choice of static rather than dynamic testing is dictated by the applicability and utility of the generated data. For a specific module, static data produce a unique structure characterization, which together with a dynamic model, can be used in a multitude of different dynamic problem situations. In contrast, dynamic force-deformation data obtained under one set of conditions cannot readily be used to predict the behavior under a different set of dynamic conditions. This is due to the fact, that in a dynamic test it is essentially impossible to separate from the data the inertial and damping effects, which change with problem dynamics, from static effects which do not, unless the static behavior is known independently. Dynamic force-deformation test data obtained for specific sets of conditions are desirable when the objective is to determine how well a specified dynamic model predicts the dynamic behavior of the module.

4.2.1.2 <u>Purpose of Specific Test Plan</u>: The purpose of the test plan is to specify test procedures, equipment and instrumentation for full-scale testing of two types of critical modules of railcars. These are the anticlimber and end sill structural subassemblage outlined in Figure 25 and the end of car superstructure outlined in Figure 26.

4.2.1.3 <u>Test Objective</u>: The objective of the tests is to determine the static force-deformation relationships for these subassemblies under a set of unidirectional loads through the full range of deformations, from load onset to full crush, as specified below.

4.2.1.4 <u>Test Conditions and Procedures</u>: <u>The anticlimber and end sill structural subassembly</u> is outlined in Figure 25. It consists of the anticlimber, the end sill assembly which extends the width of the car and forms the connection between the side sills and the bolster sill, and the bolster sill back to the reaction plane, which is rigidly fixed. The xy-coordinate system shown in the figure lies in a plane which is a plane of symmetry of the structure.
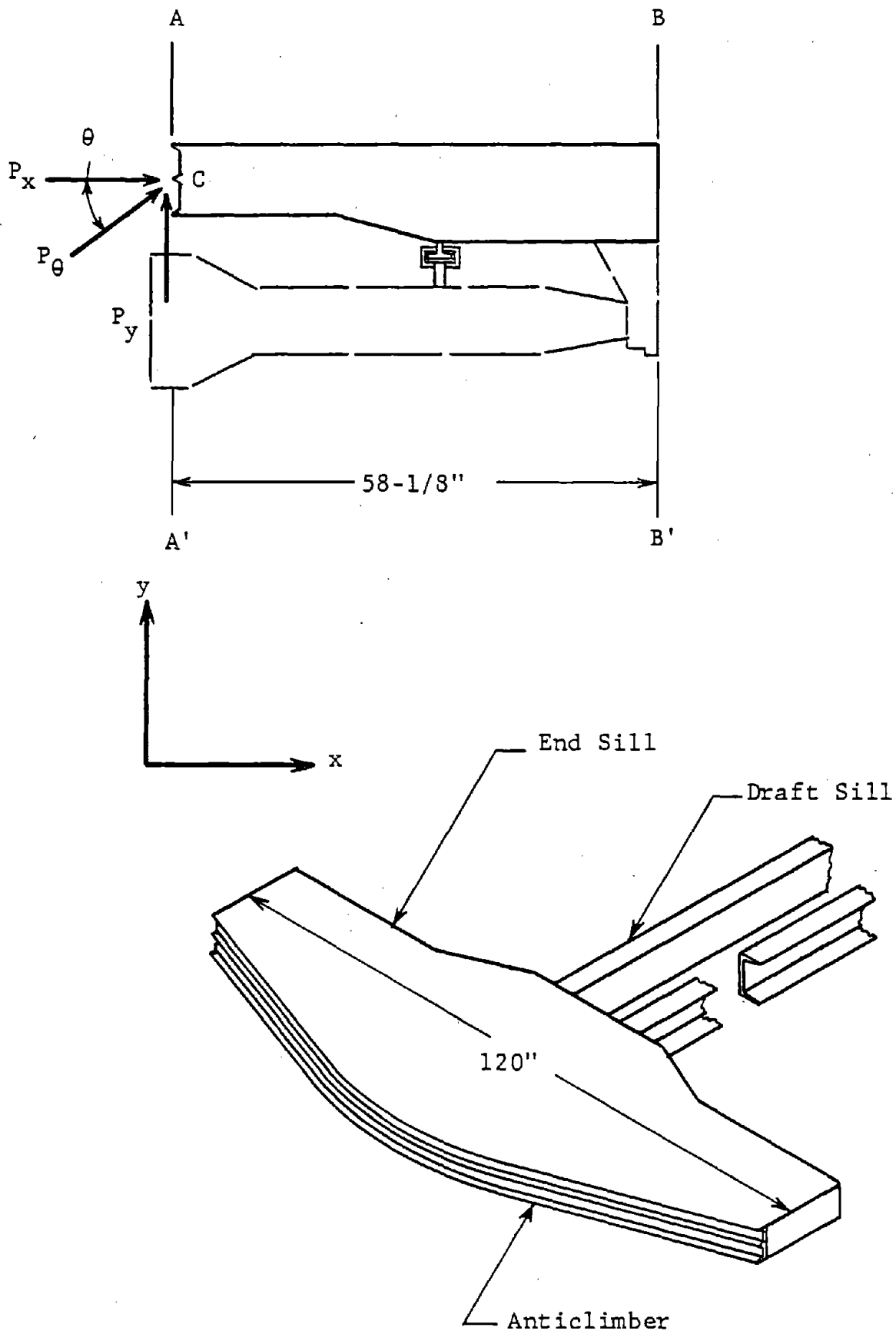
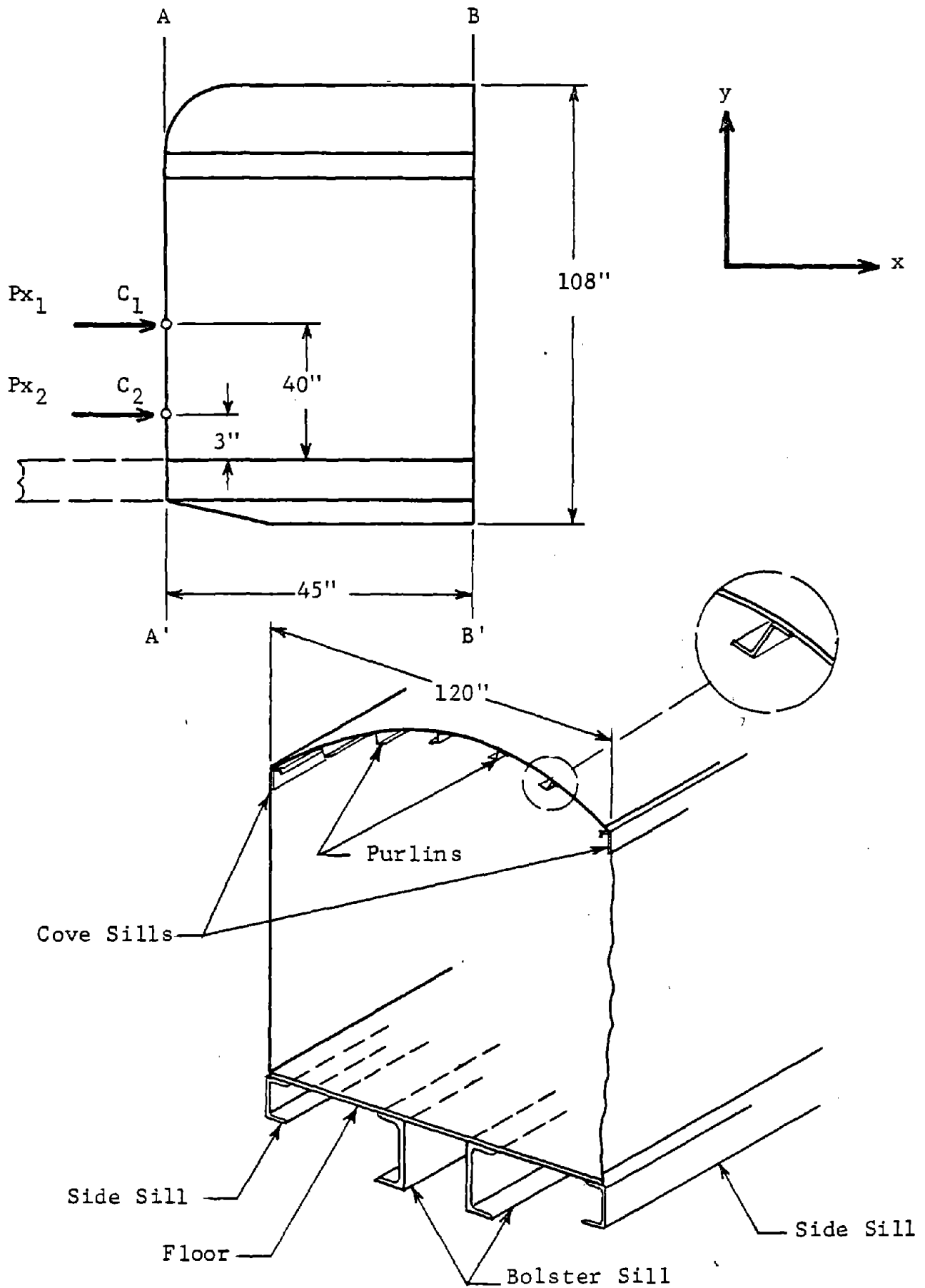FIGURE 25. ANTICLIMBER AND END SILL SUBASSEMBLY

FIGURE 26. END OF CAR SUPERSTRUCTURE SUBASSEMBLY

58

## Boundary Conditions

a. The back end of the structure, indicated as BB' in Figure 25, shall be rigidly fixed to the reaction end of the test frame to represent a fixed end condition during test.

b. The front end of the structure, indicated as AA' in Figure 25 shall be free to rotate over an axis normal to the xy-plane, but shall be restrained from moving normal to that plane.

c. The structure shall be free to expand normal to the xy-plane during test.

## Loads

a. All test loads shall be applied to the front end of the structure at the location C, in the plane of symmetry, as indicated in Figure 25.

b. Three load types will be used as shown in Figure 25. $P_X$, which is a load parallel to the x-axis, $P_y$, which is a load parallel to the y-axis, and $P_\theta$ which is a skewed load. The positive load directions are as indicated in the figure. The loads shall be maintained parallel to the indicated directions throughout the test. The direction $\theta$ shall be 45 deg to the x-axis.

c. In each test only one load type shall be used. Two tests shall be performed with each load type. A new structure shall be used for each test.

d. These maximum loads are estimated to be required to perform the tests:

$P_X$ = 1,000,000 lb

$P_y$ = 100,000 lb

$P_\theta$ = 150,000 lb

The actual loads required to complete the tests to prescribed limits of structure deformations may be smaller or larger than the above estimates.

e. The test shall terminate when either of these conditions occur:

The applied loads exceed 75 percent of specified operating loads of test machine.

The structure is crushed or has failed to such an extent that it cannot sustain a load equal to 5 percent of the maximum estimated load given in paragraph (d).

f. Load application may be intermittent in load increments, or continuous. However, the loading rate shall not exceed a structure deformation rate of 5 inches per minute in the direction of the load.

g. The load application shall be displacement controlled. This is dictated by the expected type of force-deformation behavior of the structure illustrated in Figure 27. Yield and crush of the structure will eventually force its load carrying capacity to become a decreasing function of deformation as illustrated by curve segment AB in Figure 27. If the structure starts bottoming the curve will turn up again. A displacement controlled loading device can follow the whole range of such structure deformation since the magnitude of the load on the structure is reactive to prescribed structure displacement. This is not the case with a force controlled loading device. Such a device requires a positive increment of load to produce a positive increment of deformation, and becomes a runaway (accelerating) loading system when it encounters a decreasing reaction load with increasing deformation as is the case for segment AB of the expected structure response.

Deformations

a. The displacement of the front end of the structure, at the location of the load application, shall be measured relative to the fixed back end as a function of load. The points of measurement reference at the front and back ends shall be established prior to testing.

b. The relative displacements shall be measured in two orthogonal directions; the x- and y-directions. The test shall be terminated when the displacements exceed the limits tabulated below.

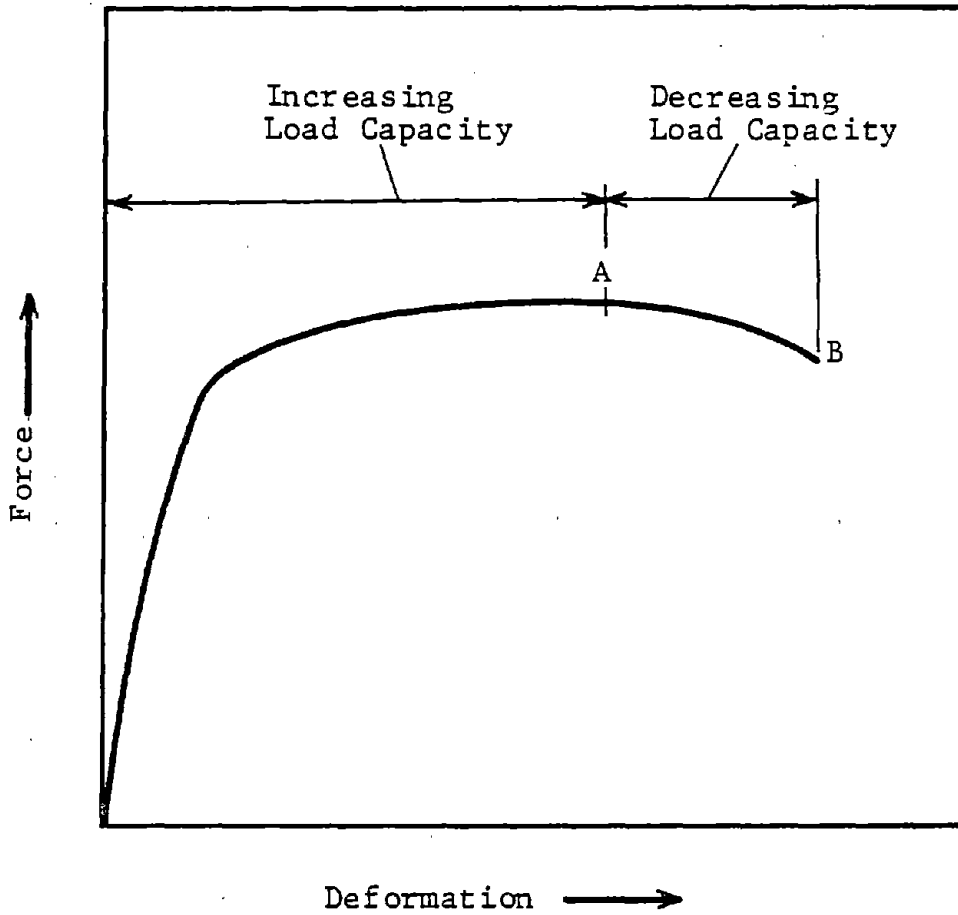| | Relative Displacement | |
| Applied Load | x-inches | y-inches |
|---|---|---|
| $P_X$ | 28 | |
| $P_y$ | | 18 |
| $P_\theta$ | 18 | 18 |

FIGURE 27.  CHARACTERISTIC LOAD-DEFORMATION BEHAVIOR
FOR A YIELDING, CRUSHING STRUCTURE

61

<u>Data</u>

    a. Force-deformation (relative displacement) response data of the structure shall be recorded during the test, from load onset to total failure as defined by the load limits or deformation limits whichever limits occur first.

    b. The data shall be acquired in a form which readily permits the construction of a force-deformation response curve such as indicated by Figure 27. Whatever method of data acquisition is used there shall be enough data to produce an unambiguous response curve.

    c. A photographic record shall be obtained of the deformed structure as a function of load or relative displacement. At least two views shall be photographed each time; normal to the x,y-plane and normal to the x,z-plane. The photorecord can be continuous, taken by motion pictures during loading, or intermittent by still pictures. In the latter case, pictures shall be taken at least every 2 inches of deformation in the applied load direction.

<u>The end of car superstructure assembly</u> is outlined in Figure 26. It consists of the roof purlins, the cove sills, the side sills, and the bolster sill. The load application points are on the collision posts, and the load is equally divided between the two posts.

The x,y-coordinate system shown in the figure lies in a plane which is a plane of symmetry of the structure. Many of the test conditions and procedures are the same as for the anticlimber and end sill structure. Nevertheless, for sake of completeness, all the conditions appropriate for the end of car superstructure subassembly are stated below.

<u>Boundary Conditions</u>

    a. The back end of the structure, indicated as BB' in Figure 26, shall be rigidly fixed to the reaction end of the test frame to represent a fixed end condition during test.

    b. The front end of the structure, indicated as AA' in Figure 26, shall be free to displace in the xy-plane. It shall also be free to rotate over an axis normal to the xy-plane, but shall be restrained from moving normal to that plane.

c. The structure shall be free to expand normal to the xy-plane during test.

## Loads

a. All test loads shall be applied to the front end of the structure at location $C_1$ and $C_2$, in the plane of symmetry, as indicated in Figure 26.

b. Two load types, $P_{X1}$ and $P_{X2}$, will be used in the tests. These loads are parallel to the x-axis and their positive directions are as indicated in Figure 26. The loads shall be maintained parallel to the indicated directions throughout the test.

c. In each test only one load type shall be used. Two tests shall be performed with each load type. A new structure shall be used for each test.

d. These maximum loads are estimated to be required to perform the tests:

$$P_{X1} = 150,000 \text{ lb}$$

$$P_{X2} = 150,000 \text{ lb}$$

The actual loads required to complete the tests to prescribed limits of structure deformations may be smaller or larger than the above estimates.

e. The test shall terminate when either of these conditions occur:

The applied loads exceed 75 percent of specified operating loads of test machine.

The structure is crushed or has failed to such an extent that it cannot sustain a load equal to 5 percent of the maximum estimated load given in paragraph (d).

f. Load application may be intermittent in load increments, or continuous. However, the loading rate shall not exceed a structure deformation rate of 5 inches per minute in the direction of the load.

g. The load application shall be displacement controlled. This is dictated by the type of force-deformation behavior of the structure which is expected to have the characteristics illustrated in Figure 27.

## Deformations

a. The displacement of the front end of the structure, at the location of the load application, shall be measured relative to the fixed back end as a function of load. The points of measurement reference at the front and back ends shall be established prior to testing.

63

b. The relative displacements shall be measured in two orthogonal directions, the x- and y-directions. The test shall be terminated when the displacements exceed the limits tabulated below.

| Applied Load | Relative Displacement | |
| --- | --- | --- |
| | x-inches | y-inches |
| $P_{X1}$ | 20 | 12 |
| $P_{X2}$ | 20 | 12 |

Data

a. Force-deformation (relative displacement) response data of the structure shall be recorded during the test, from load onset to total failure as defined by the load limits of deformation limits whichever limits occur first.

b. The data shall be acquired in a form which readily permits the construction of a force-deformation response curve such as indicated by Figure 27. Whatever method of data acquisition is used there shall be enough data to produce an unambiguous response curve.

c. A photographic record shall be obtained of the deformed structure as a function of load or relative displacement. At least two views shall be photographed each time; normal to the xy-plane and normal to the xz-plane. The photorecord can be continuous, taken by motion pictures during loading, or intermittent by still pictures. In the latter case, pictures shall be taken at least at every 2 inches of deformation in the applied load direction.

4.2.1.5 Test Equipment: The test equipment to be used to perform the tests specified in Section 4.2.1.4 shall consist of a test frame, load unit, instrumentation, and data acquisition system.

In the specification to follow, the three basic orthogonal directions will be referred to as longitudinal, transverse and normal, with the corresponding coordinate axes designated $\ell$, t and n. The coordinate axes $\ell$ and t are coplanar with the axes x and y of Figures 25 and 26 and n is codirectional with the z axis of

these figures.   Directionally subscripted parameters refer to parameters in the subscripted direction.

Structural Test Frame

a. All loads arising from the test must be reacted entirely within the structural test frame. The frame and its foundation must be capable of supporting the deadweight of the test specimen.

b. The frame must be sufficiently stiff to permit application of load without introducing measurement errors in the deformation of the test specimen or applied load greater than 1 percent of the measurement being performed.

c. The frame shall permit bolting or welding of the back end of the specimen to it, to create a fixed end condition.  This capability must be available for three specimen orientations relative to the frame longitudinal axis $\ell$ as follows:  For the specimen x-axis codirectional with $\ell$, for the specimen y-axis codirectional with $\ell$, and for the specimen $\theta$-orientation (Figure 25) codirectional with $\ell$.  This approach reduces the test equipment requirements to a system with only one powered load application direction.

d. The frame shall have an unobstructed space to accommodate the test specimen between the end to which the specimen will be fixed and the crosshead and fixtures applying the load.  This unobstructed space shall have these minimum dimensions:

$L_\ell$ = 5 ft 6 inches

$L_t$ = 12 ft

$L_n$ = 12 ft

e. The frame must permit unobstructed deformation of the test specimen during test.  The maximum deformations for each test condition are given in Section 4.2.1.4.

f. The frame must provide a sufficient unobstructed view to permit the photographing of the deformed state of the specimen during test.  Two views will be photographed; in the t-direction and n-direction in accordance with the requirements of Section 4.2.1.4.

65

## Load Unit

a. The load unit shall have a crosshead guided to move in the longitudinal direction of the test frame and be reacted by the test frame against side motion.

b. The crosshead shall deliver the test load to the test specimen in the longitudinal direction. Load transfer from the crosshead to the specimen shall be via two fixtures; an articulation head and a load transfer pad.

c. The articulation head will interface with the crosshead. The interface and articulation head will be designed to perform the following functions: They will permit the specimen load-end to freely hinge or roll to simulate a hinged end. They will permit the specimen load-end to move freely in the transverse direction but restrain specimen motion in the normal direction. To accomplish these objectives, the interface and articulation head shall be designed to have as low as practical frictional restraint forces in the direction of desired free motion (transverse, hinge and/or roll).

d. The load transfer pad shall interface with the articulation head and the load-end of the specimen. Its function shall be to provide a prescribed load distribution on the load-end of the specimen during load application. Since requirements may vary between tests, or the pad may suffer damage during test, the pad shall be an interchangeable or disposable item.

e. To perform the tests described in Section 4.2.1.4, the crosshead shall have the capacity to deliver to the specimen, in the longitudinal direction, loads in a pushing mode ranging from zero up to these operating maximum loads:

$P_1$ = 2,000,000 lb

$P_2$ =  200,000 lb

$P_3$ =  300,000 lb

The load application capacity may be intermittent in load increments, or continuous. The smallest incrementation capability shall be no greater than the load measuring accuracy of the load cell or the load reading resolution, whichever is smaller.

f. The crosshead shall be powered by a power unit of sufficient capacity to provide the loads called for in paragraph (e) and overcome any extraneous resisting loads generated in the load transfer system between the power unit and the crosshead.

g. The load transfer system to the crosshead shall be of the displacement control type. This can be accomplished by using a screw advance system.

h. The crosshead shall be capable of loading the specimen at one or more crosshead displacement rates in the range of up to 5 inches per minute.

i. To perform the tests specified in Section 4.2.1.4 the crosshead shall have all of the minimum displacement capabilities listed below. These shall be relative to the fixed end of the specimen.

| Specimen Load Type | Minimum Required Crosshead Displacements (inch) | | |
|---|---|---|---|
| | Initial Free | Powered | Total |
| $P_x$ | 6 | 28 | 34 |
| $P_y$ | 6 | 18 | 24 |
| $P_\theta$ | 6 | 26 | 32 |
| $P_{x_1}, P_{x_2}$ | 6 | 20 | 26 |

j. The articulation head, conforming to its function described in paragraph (c) shall permit a minimum of 30 inches of free transverse motion and 90 deg of rotation about the normal axis.

Instrumentation

a. The test machine shall be equipped with a suitable load measuring system, for instance, one or more load cells, to accurately and continuously measure the load applied to the test specimen in the longitudinal direction. The system shall be capable of measuring the applied loads with these minimum accuracies:

| Measuring Range, lb | | Accuracy |
|---|---|---|
| Lower Limit | Upper Limit | Percent of Upper Limit |
| 0 | 250,000 | $\pm$ 0.5 |
| 250,000 | 500,000 | $\pm$ 0.5 |
| 500,000 | 1,000,000 | $\pm$ 0.5 |
| 1,000,000 | 2,000,000 | $\pm$ 0.5 |

b. The test machine shall be equipped with a displacement measuring system to accurately and continuously measure during testing the displacement of the load end of the specimen relative to its fixed end. These measurements shall be in the longitudinal and trans- verse directions. The system shall be capable of measuring the displacements with a minimum accuracy of 0.05 inch in the above two directions, each of which shall have a range of 36 inches.

## Data Acquisition and Monitoring System

a. The load and displacement measuring systems of the test machine shall be provided with suitable signal conditioning to enable the continuous and simultaneous monitoring of the specimen load and displacement during the test.

b. A compatible automatic data recording system shall be part of the measuring system. It shall be capable of recording simultaneously the monitored loads and displacements with these minimum resolutions:

Displacements: 0.025 inch

| Loads: | Measuring Range, lb | Resolution, lb |
|---|---|---|
| | 0 - 250,000 | 500 |
| | 250,000 - 500,000 | 1000 |
| | 500,000 - 1,000,000 | 2000 |
| | 1,000,000 - 2,000,000 | 4000 |

c. The data recording system shall as a minimum provide digital and/or graphical recording modes. It shall also simultaneously visually display these modes at a location convenient for supervision and control of the ongoing test. The system shall also provide for optional magnetic tape recording of the data during test.

## Control and Safety

a. Necessary crosshead loading and displacement control mechanisms shall be incorporated into the test machine system to permit the operator to perform the tests required in Section 4.2.1.4. This shall include but not be limited to:

   Presetting of load and displacement limits as required by test specification.

   Automatic stoppage and/or system shutdown when test limits are reached.

Manual override of these limits.

Manual load and/or displacement incrementation, restart and stop.

b. Fail-safe features shall be provided to prevent equipment damage. They will override the test program in the event of specimen failure or incorrect operation. They will also provide stop or load dumping for the following minimum occurrences.

Test machine parameters reach preset limits.

Operator actuates emergency controls.

c. Other automatic fail-safe systems shall be incorporated in the test machine as deemed necessary.

4.2.1.6 <u>Test Equipment Feasibility</u>: The test equipment specifications given in the previous section are all well within the present state of the art for commercially available mechanical components. Therefore the design and construction of such a test machine is both feasible and within the state of the art. Examples of applicable components are screw jacks and low friction precision ball bearing screws, with capacities from thousands to millions of pounds. They are available from several sources[*] as components to power and guide the machine crosshead. Likewise, load cells with capacities ranging into millions of pounds are available[**] as components to measure the test loads.

There may be in existence presently, test machines with both the physical size and capacity to perform the recommended railcar module tests. The finding and utilization of such a machine or machines should be looked into as a viable alternative to building a new machine. A source of information for this purpose is the National Bureau of Standards which has initiated a national referral service for organizations requiring high-capacity mechanical testing (Ref. 4).

---

[*] Pow-R-Jacs. Division, Limitorque Corp., King of Prussia PA 19406

Waruer Electric Brake & Clutch Company, Beloit WI 53511

Saginaw Steering Gear Division, General Motors Corp., Saginaw MI 48605

[**] Lebow Associates, Inc., 1728 Maplelawn Road, Troy MI 48084

BLB Electronics, Inc., 42 Fourth Ave., Waltham MA 02154

NBS personnel are presently compiling for the "Mechanical and Structural Testing and Referral Service" (MASTARS), a comprehensive MASTAR File of all for-hire United States mechanical-testing facilities with capacities exceeding 1 million pounds. The service parallels and strengthens the testing and research program which NBS previously offered, based on its 12 million pound universal testing machine.

Large size and capacity test machines may also be present at several United State universities. For instance the Department of Engineering Mechanics at the University of Wisconsin has such a multimillion pound test machine.

Lastly, as another alternative, it may be possible to convert a common car crushing machine, as presently used by many United States car disposal junk yards, into the desired test machine.

4.2.2 <u>Scale Model Tests</u> - A third procedure which might be attempted to obtain force-deformation data for structural subassemblages would be scale model testing. As in the finite element procedures and full-scale testing previously described, static data would need to be obtained to use in a computer code for the dynamic simulation of transit car collisions. Since large deflections of the structure are to be simulated any scale model would be required to provide valid data in both the elastic and plastic range. This requirement places great limitations on the use of scale modeling for complex structures such as transit cars. In order that the scale model accurately predict force-deformation data, the model materials must scale both the elastic and plastic behavior of the structure. This normally would require that the structure and the model be composed of identical materials.

Let us investigate a model having a geometric scaling factor $K_g$. Then

$$L_m = K_g L_s$$

where L is a characteristic length and the subscripts m and s refer to the model and the structure, respectively. If the model and the structure are composed of identical materials, the stresses in the model and structure should also be identical to ensure valid scaling in both the elastic and plastic range. Therefore,

$$\sigma_m = \sigma_s$$

Stress is given by an equation of the form

$$\sigma = P/L^2$$

where P is the load and L is the proper characteristic length. Equating the stresses for the model and the structure

$$P_m/L_m^2 = P_s/L_s^2$$

Utilizing the first of the above equations and solving for the model loading

$$P_m = (K_g^2) \, P_s = K_p \, P_s$$

where the scaling factor for forces, $K_p$, is equal to the square of the geometric scaling factor. Deflection is given by an equation of the form

$$\delta = ( \sigma'/E' + \sigma''/E'') \, L$$

or
$$\delta/L = ( \sigma'/E' + \sigma''/E'')$$

where $\sigma'$ and $E'$ are the elastic stress and modulus, $\sigma''$ and $E''$ are the plastic stress and modulus, and L is the proper characteristic length. Since the stresses and material moduli are identical for the model and the structure

$$\delta_m/L_m = \delta_s/L_s$$

and
$$\delta_m = (L_m/L_s)\delta_s = K_g \, \delta_s = K_\delta \, \delta_s$$

where the scaling factor for deflections, $K_\delta$, is equal to the geometric scaling factor.

With the scaling factors for force and deflection known, a geometric scale model of a transit car structural subassembly can be structured and tested and the force-deflection characteristics of the full-scale structure can be estimated. The testing techniques used would be similar to the full-scale tests described previously except size and force requirements would be reduced in accordance with the scaling factors derived here.

## 5. REFERENCES

1. Yeung, K. S. and Welch, R. E., "Refinement of Finite Element Analysis of Sheet Metal in Vehicle/Pedestrian and Vehicle/Vehicle Collisions," Final Report, DOT Contract DOT-HS-6-01364, IITRI Project J6384, August 1977.

2. Newmark, N. M., "A Method of Computation for Structural Dynamics," J. Engr. Mech. Div., ASCE, Vol. 85, EM3, July 1959.

3. Mallet, R. H. and Haftka, R. T., "Progress in Nonlinear Finite Element Analysis Using Asymptotic Solution Techniques," Second U.S.-Japan Seminar on Matrix Methods, 1972.

4. MASTARS, EM219, National Bureau of Standards, Washington, DC 20234.